

Kmenové buňky a hierarchická organizace tkání demonstrována na příkladu epitelu střeva

Vítězslav Bryja

Kmenové buňky

► Pro zájemce o tuto problematiku:

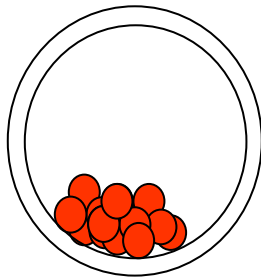
Dr. Jiří Pacherník: Bi7575 Biologie kmenových buněk

Kmenové buňky

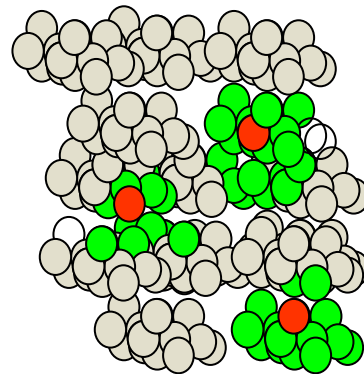
Základní vlastnosti:

- a) sebeobnova (**selfrenewal**)
 - b) multipotence – schopnost dávat vznik dalším buněčným typům
- tkáňově specifické
 - embryonální kmenové (embryonic stem cells, ES)

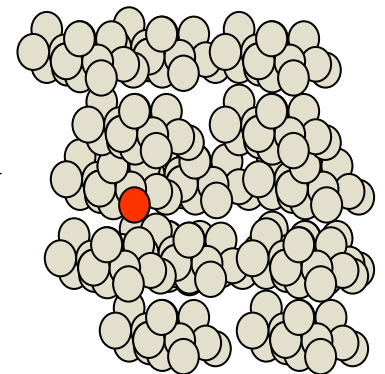
blastocysta



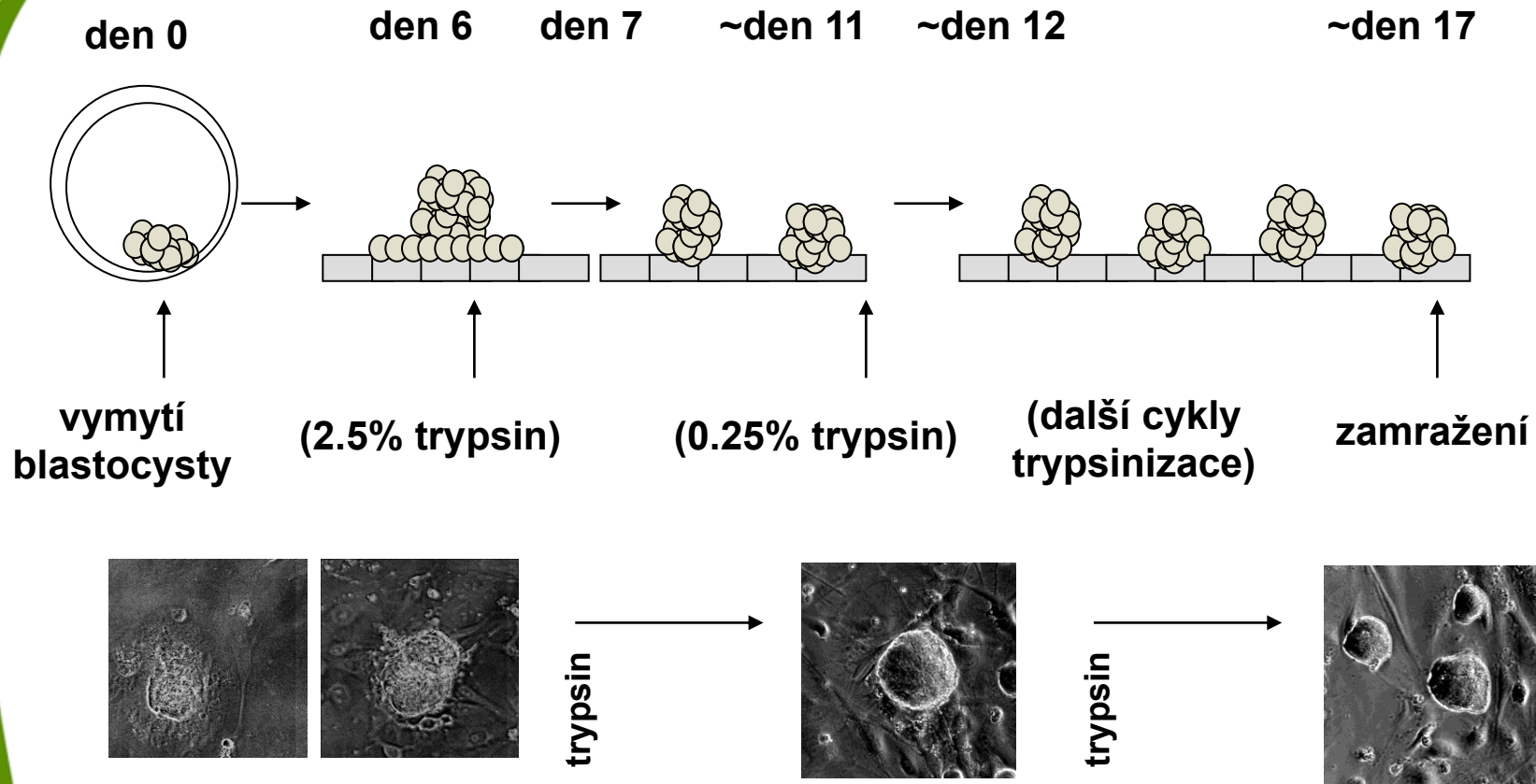
vyvíjející se tkáň (orgán)



dospělá tkáň



Příprava myších embryonálních kmenových buněk:



Nutná přítomnost proteinu LIF (leukemia inhibitory factor) a podpurné vrstvy MEF (mouse embryonal fibroblast) buněk

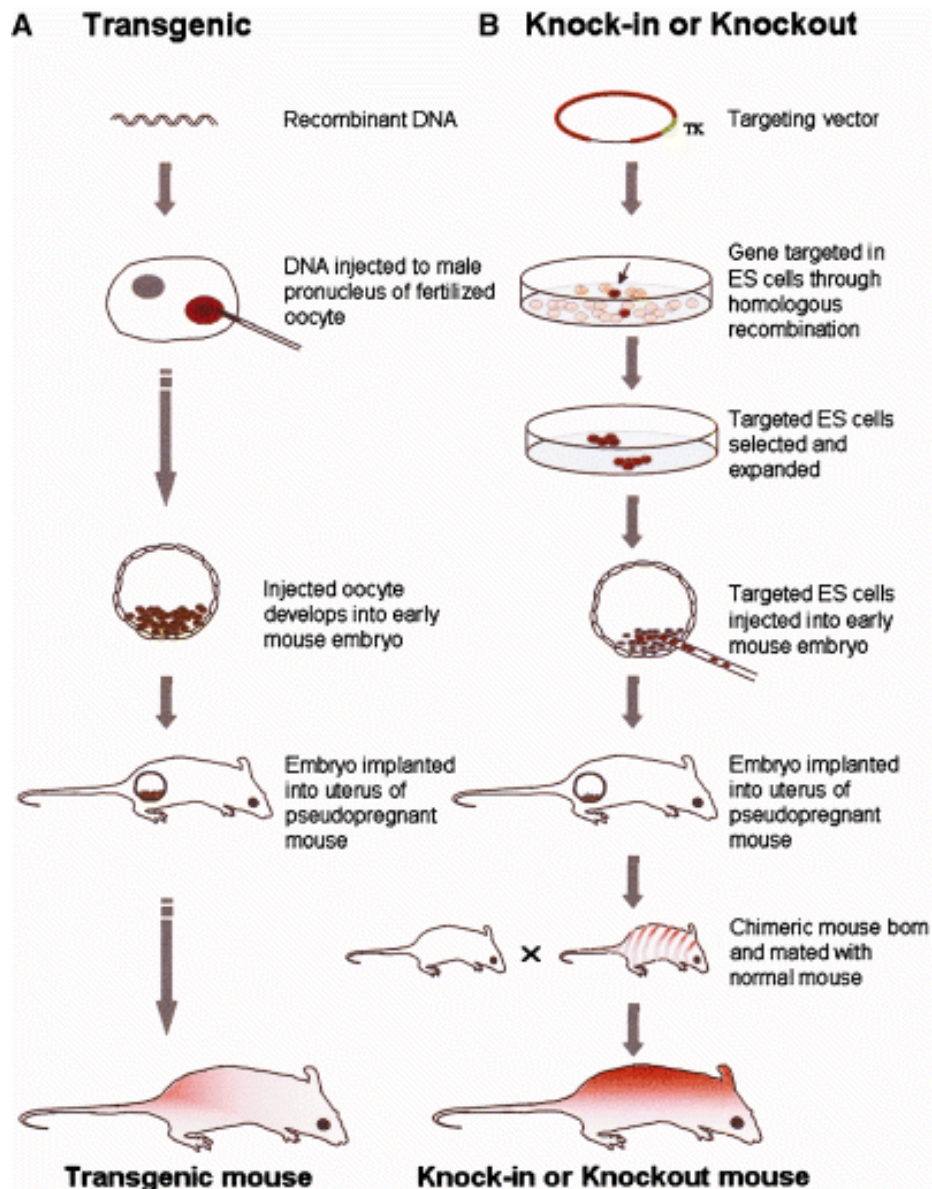
Využití myších ES buněk pro transgenezi

Nobelova cena 2007

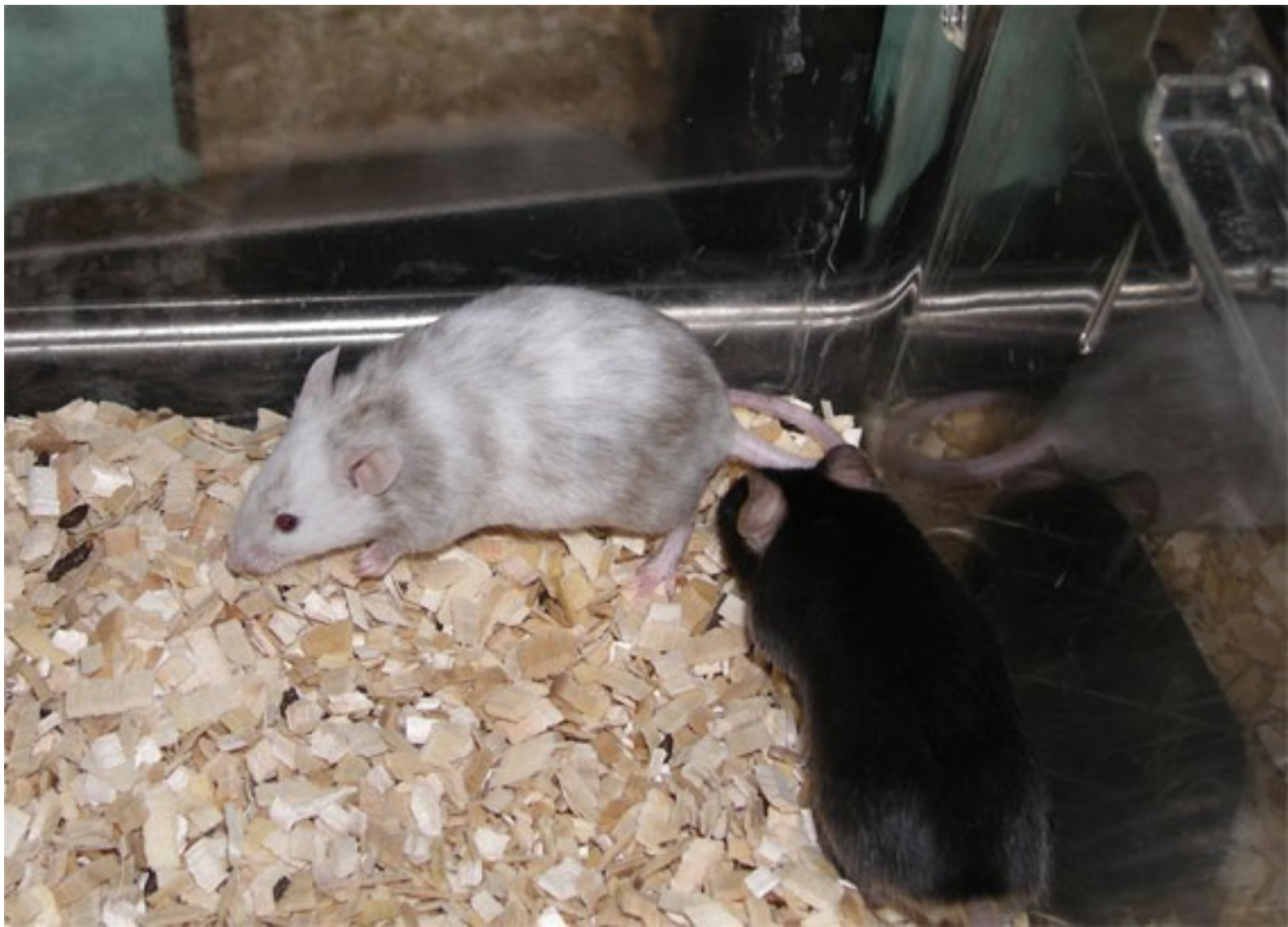
**Mario R. Capecchi,
Martin J. Evans and
Oliver Smithies**

za

„principles for
introducing specific
gene modifications in
mice by the use of
embryonic stem cells“



Využití myších ES buněk pro transgenezi



REPORTS

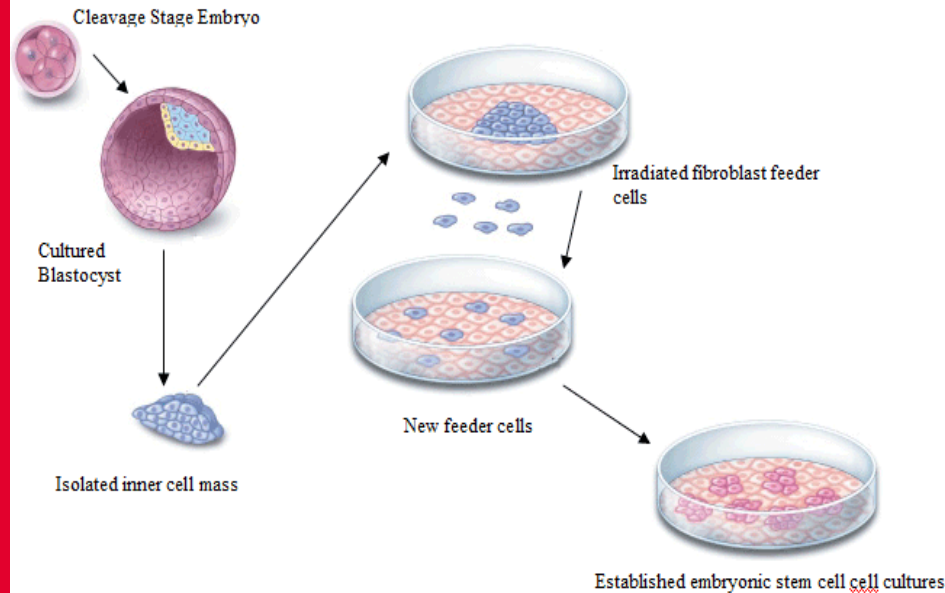
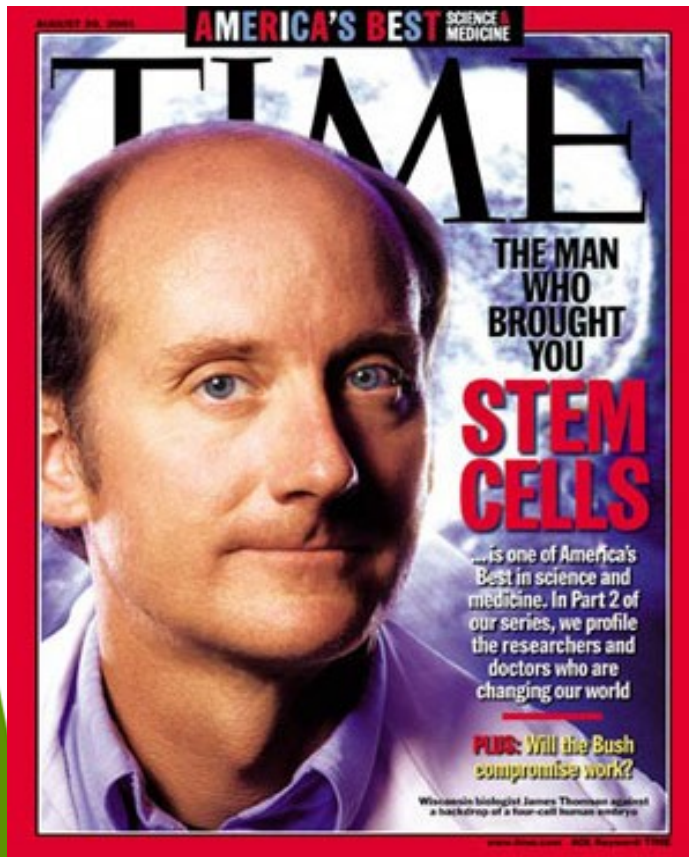
Embryonic Stem Cell Lines Derived from Human Blastocysts

James A. Thomson,* Joseph Itskovitz-Eldor, Sander S. Shapiro, Michelle A. Waknitz, Jennifer J. Swiergiel, Vivienne S. Marshall, Jeffrey M. Jones

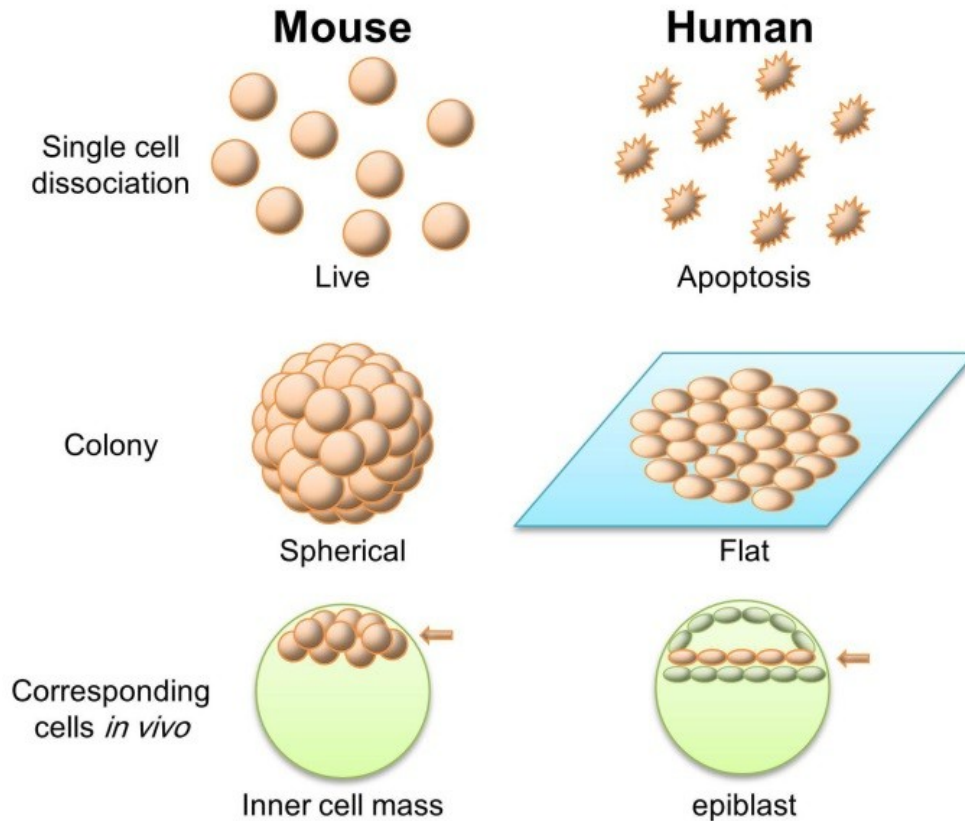
XX karyotype after 6 months of culture and has now been passaged continuously for more than 8 months (32 passages). A period of replicative crisis was not observed for any of the cell lines.

The human ES cell lines expressed high levels of telomerase activity (Fig. 2). Telomerase is a ribonucleoprotein that adds telomere repeats to chromosome ends and is involved in maintaining telomere length, which plays an important role in replicative

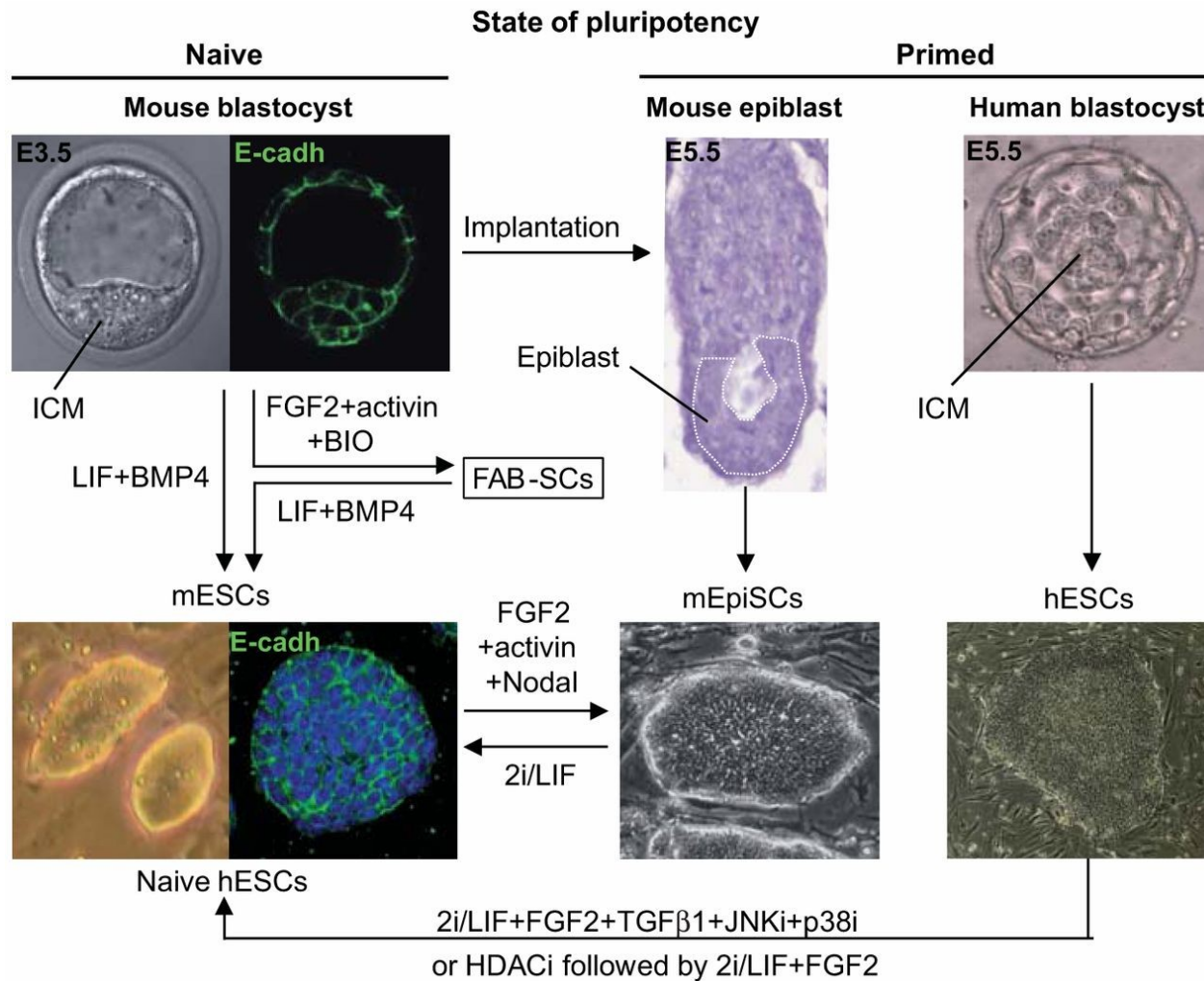
Science. 1998 Nov 6;282(5391):1145-7



Rozdíly mezi myšimi a lidskými ES buňkami



Naive and primed pluripotency states of embryos and stem cells

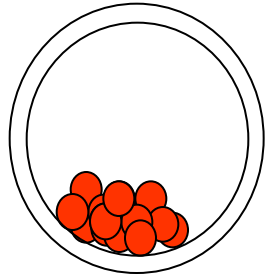


Tim Pieters, and Frans van Roy J Cell Sci 2014;127:2603-2613

Naive and primed pluripotency states of embryos and stem cells. ICM cells from mouse blastocysts and their *in vitro* counterpart, mESCs, represent the ground (naive) state of pluripotency. These naive stem cells express E-cadherin (E-cadh) both *in vivo* and *in vitro*. After implantation, epiblast cells are organized into a cup-shaped epithelium, from which mEpiSCs can be isolated. Both mEpiSCs and hESCs depend on FGF2+activin+Nodal signaling and represent primed states of pluripotency. Also, primed SCs – called FAB-SCs – can be isolated from blastocysts when treated with FGF2, activin and the glycogen synthase kinase 3 inhibitor BIO. Pluripotency states display plasticity and, by providing appropriate signals when, e.g. using specific inhibitors (2i) and cytokines, different types of primed stem cell (i.e. mEpiSCs, FAB-SCs and hESCs) can be converted to naive stem cells. Images of the human blastocyst and hESC colony are courtesy of Petra De Sutter and Katrien De Mulder (both at Ghent University), respectively.

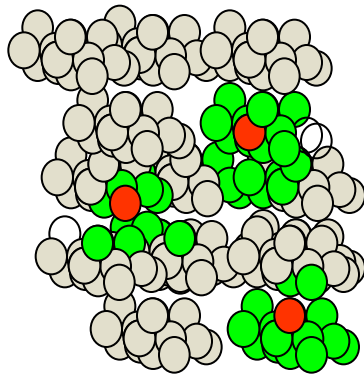
embryonální vývoj

In vivo

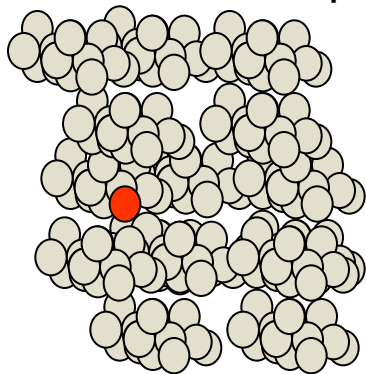


blastocysta

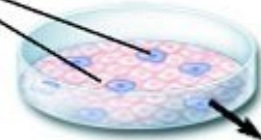
vyvíjející se tkáň (orgán)



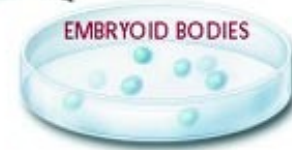
dospělá tkáň



In vitro



Undifferentiated embryonic stem cells



EMBRYOID BODIES

IIFSn medium (insulin/transferrin/fibronectin/selenium)

Adherent substrate

SELECTION OF NESTIN-POSITIVE CELLS

N2 medium/bFGF/aminin

N2 medium/bFGF/
B27 media supplement

Expansion Phase

NESTIN-POSITIVE NEURONAL
PRECURSOR CELLS

NESTIN-POSITIVE PANCREATIC
PROGENITOR CELLS

Remove bFGF

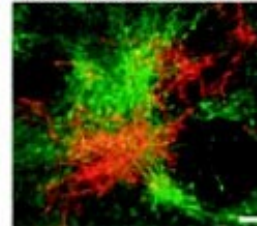
Differentiation Phase

Remove bFGF
Add nicotinamide

DOPAMINE- AND SEROTONIN-
SECRETING NEURONS

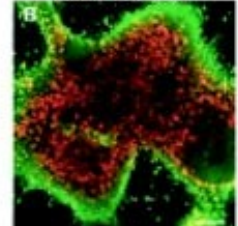
INSULIN-SECRETING PANCREATIC
ISLET-LIKE CLUSTERS

TYROSINE HYDROXYLASE/SEROTONIN



Reproduced with permission from Nature Biotechnology

INSULIN/GLUCAGON



Reproduced with permission from Science

Induction of Pluripotent Stem Cells from Mouse Embryonic and Adult Fibroblast Cultures by Defined Factors

Kazutoshi Takahashi¹ and Shinya Yamanaka^{1,2,*}

¹Department of Stem Cell Biology, Institute for Frontier Medical Sciences, Kyoto University, Kyoto 606-8507, Japan

²CREST, Japan Science and Technology Agency, Kawaguchi 332-0012, Japan

*Contact: yamanaka@frontier.kyoto-u.ac.jp

DOI 10.1016/j.cell.2006.07.024

SUMMARY

Differentiated cells can be reprogrammed to an embryonic-like state by transfer of nuclear contents into oocytes or by fusion with embryonic stem (ES) cells. Little is known about factors that induce this reprogramming. Here, we dem-

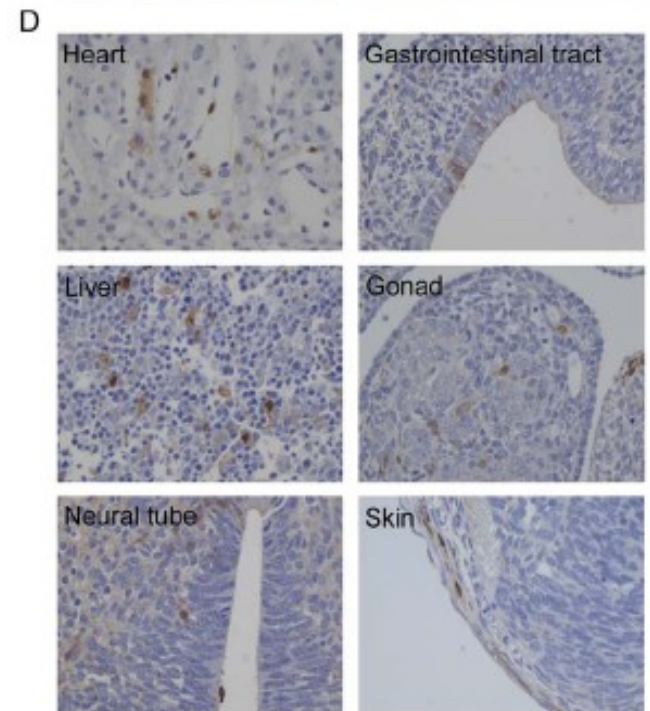
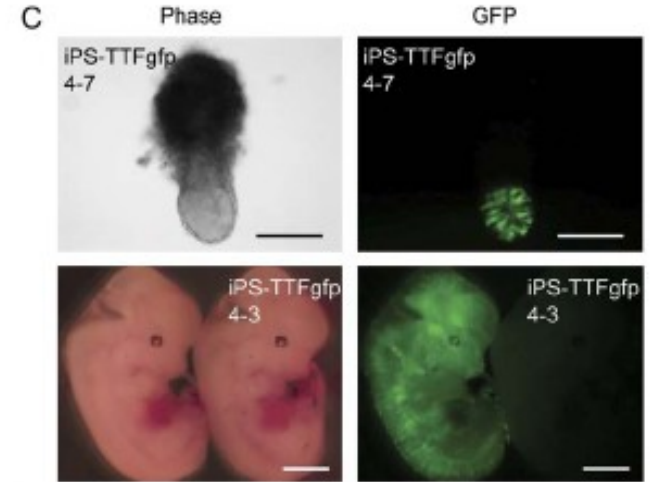
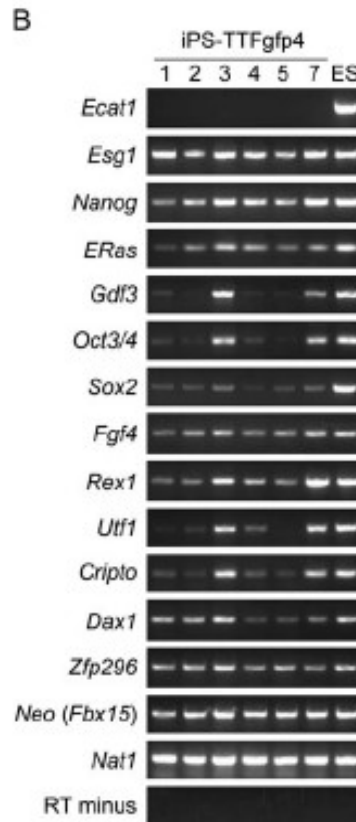
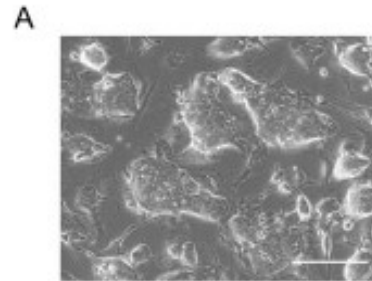
onstrated that unfertilized eggs and ES cells contain factors that can confer totipotency or pluripotency to somatic cells. We hypothesized that the factors that play important roles in the maintenance of ES cell identity also play pivotal roles in the induction of pluripotency in somatic cells.

iPSCs: Buňky s vlastnostmi embryonálních kmenových buněk, které byly připraveny tzv. přímým reprogramováním kombinací transkripčních faktorů

Indukované kmenové buňky - iPSCs

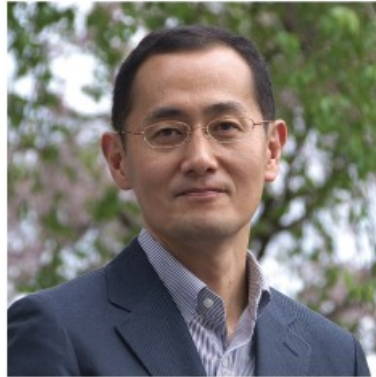


Oct3/4
 Sox2
 c-Myc
 Klf4



Indukované kmenové buňky - iPSCs

2012 Nobel Prize in Physiology or Medicine

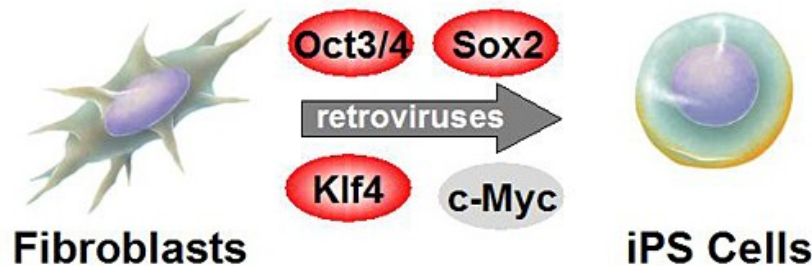


Shinya Yamanaka
University of Kyoto, Japan
*Photo Credit:
Center for iPS cell Research and Application, Kyoto University*



John B. Gurdon
Gurdon Institute in Cambridge, UK

Induced Pluripotent Stem (iPS) Cells

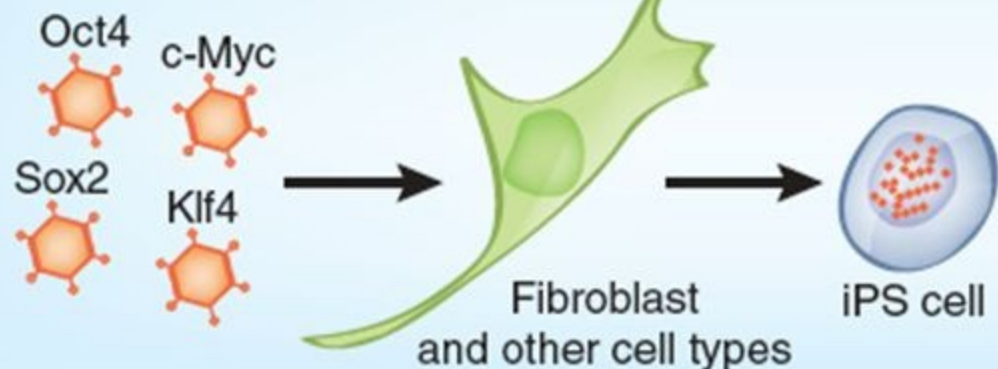


Mouse iPS cells reported in 2006

Human iPS cells reported in 2007

The many ways to make an iPS Cell

Retroviral or lentiviral transduction



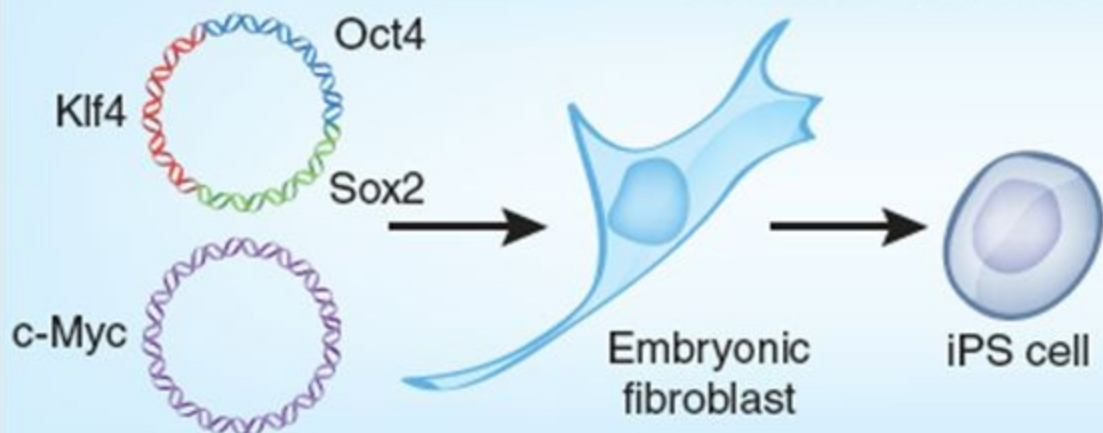
Genomic integration

Tumors in chimeric animals due to ectopic expression of proviral transgenes

Perinatal death of hepatocyte-derived iPS chimera

C

Plasmid transfection



No genomic integration

Future goal is eliminate as many of the K,O,S,M factors as possible and replace them with small molecules

Direct reprogramming – přímé přeprogramování

Proces, kterým lze s použitím kombinace transkripčních faktorů (nebo inhibitorů/aktivátorů signálních drah) změnit jeden buněčný typ v druhý.

Např. gliové buňky v dopaminergní neurony:

ARTICLES

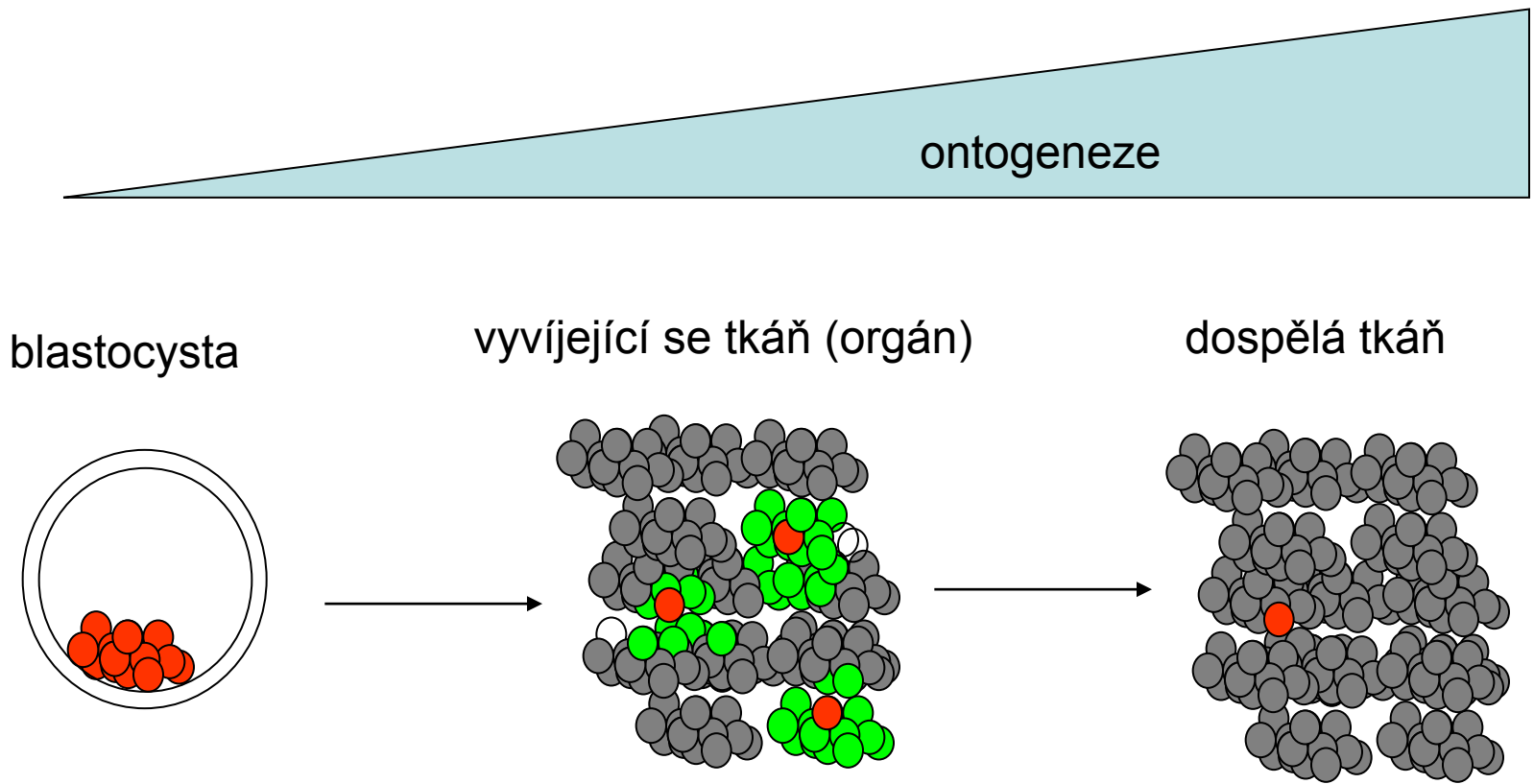
nature
biotechnology

Induction of functional dopamine neurons from human astrocytes *in vitro* and mouse astrocytes in a Parkinson's disease model

Pia Rivetti di Val Cervo¹, Roman A Romanov^{2,3}, Giada Spigolon³, Débora Masini³, Elisa Martín-Montañez^{1,4}, Enrique M Toledo¹, Gioele La Manno¹, Michael Feyder³, Christian Pifl², Yi-Han Ng⁵, Sara Padrell Sánchez¹, Sten Linnarsson¹, Marius Wernig⁵, Tibor Harkany^{2,3}, Gilberto Fisone³ & Ernest Arenas¹

Cell replacement therapies for neurodegenerative disease have focused on transplantation of the cell types affected by the pathological process. Here we describe an alternative strategy for Parkinson's disease in which dopamine neurons are generated by direct conversion of astrocytes. Using three transcription factors, NEUROD1, ASCL1 and LMX1A, and the microRNA miR218, collectively designated NeAL218, we reprogram human astrocytes *in vitro*, and mouse astrocytes *in vivo*, into induced dopamine

Kmenové buňky



K čemu jsou, jak vypadají a jak jsou regulovány kmenové buňky v dospělém organismu?

K čemu jsou tkáňově specifické kmenové buňky?

- 1) K zajištění homeostázy
 - v lidském organismu se průběžně obnovují celé tkáně – např. vlasové kořínky (doba „života“ 3-4 roky), epitel střeva, epitel plic, krevní buňky nebo játra
- 2) K zajištění procesu hojení a regenerace

Časy – délka „života“ buněk

cell type	turnover time	BNID
small intestine epithelium	2–4 days	107812, 109231
stomach	2–9 days	101940
blood neutrophils	1–5 days	101940
white blood cells eosinophils	2–5 days	109901, 109902
gastrointestinal colon crypt cells	3–4 days	107812
cervix	6 days	110321
lungs alveoli	8 days	101940
tongue taste buds (rat)	10 days	111427
platelets	10 days	111407, 111408
bone osteoclasts	2 weeks	109906
intestine paneth cells	20 days	107812
skin epidermis cells	10–30 days	109214, 109215
pancreas beta cells (rat)	20–50 days	109228
blood B cells	1 month	111516
trachea	1–2 months	101940
hematopoietic stem cells	2 months	109232
sperm (male gametes)	2 months	110319, 110320
bone osteoblasts	3 months	109907
red blood cells	4 months	101706, 107875
liver hepatocyte cells	0.5–1 year	109233
fat cells	8 years	103455
cardiomyocytes	0.5–10% per year	107076, 107077, 107078
central nervous system	life-time	101940
skeleton	10% per year	109908
lens cells	life-time	109840
oocytes (female gametes)	life-time	111451

Jak zjistit délku „života“ buněk/intenzitu obnovy tkání?

Využití přechodného zvýšení ^{14}C z dob studené války
(Jonas Frisén, Karolinska)

Nervové buňky mozkové kůry

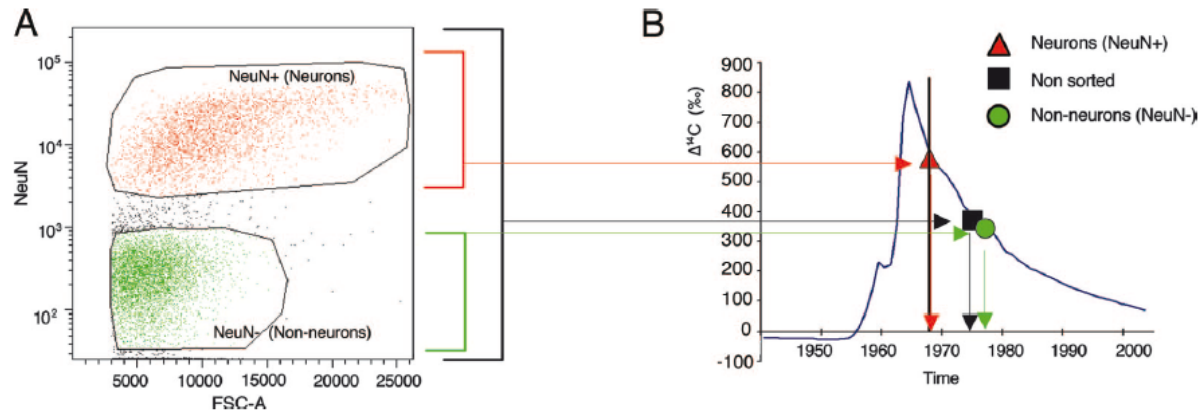


Fig. 1. Determination of the age of neocortical neurons. (A) Neuronal (NeuN-positive) and nonneuronal (NeuN-negative) cell nuclei from the adult human cerebral neocortex were separated and isolated by flow cytometry. (B) The levels of ^{14}C in the atmosphere have been stable over long time periods, with the exception of a large addition of ^{14}C in 1955–1963 as a result of nuclear weapons tests (blue line, data from ref. 26), making it possible to infer the time of birth of cell populations by relating the level of ^{14}C in DNA to that in the atmosphere (horizontal arrows) and reading the age off the x axis (vertical arrows). The average age of all cells in the prefrontal cortex is younger than the individual (black arrows), indicating cell turnover. Dating of nonneuronal cells demonstrates they are younger, whereas neurons are approximately as old as the individual. The vertical bar indicates the year of birth of the individual. ^{14}C levels from modern samples are, by convention, given in relation to a universal standard and corrected for radioactive decay, giving the $\Delta^{14}\text{C}$ value (50).

(Ne)Dynamika srdečních svalových buněk

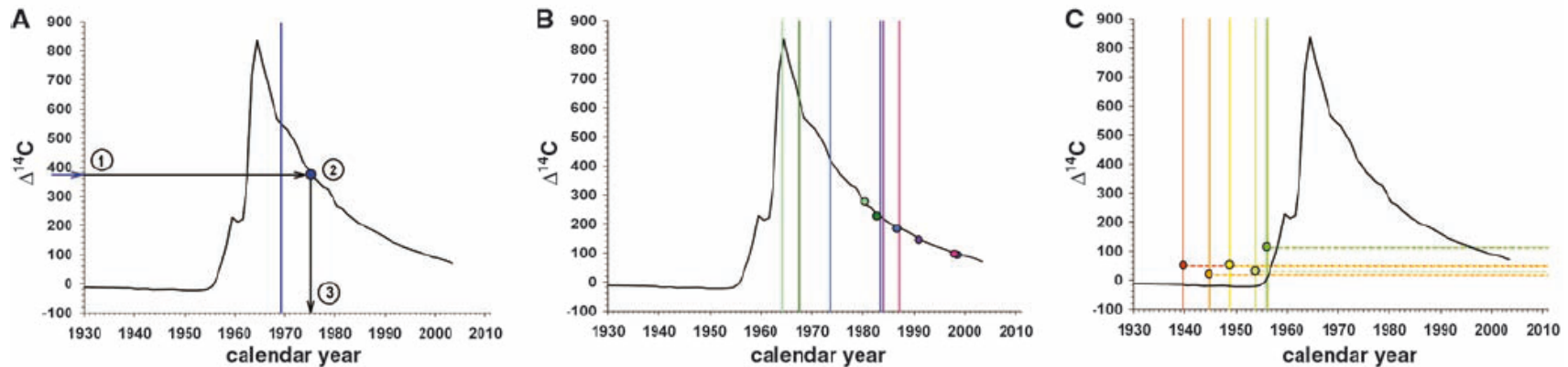
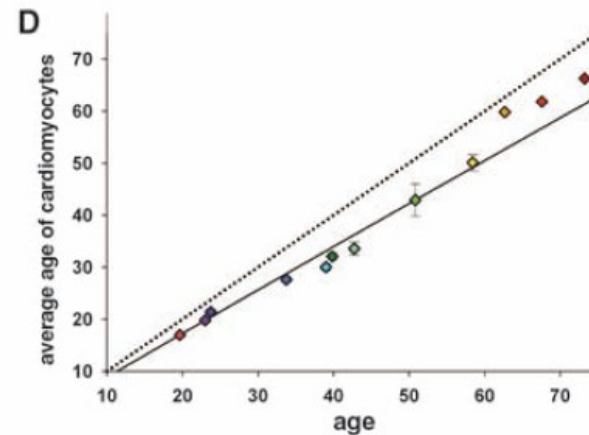
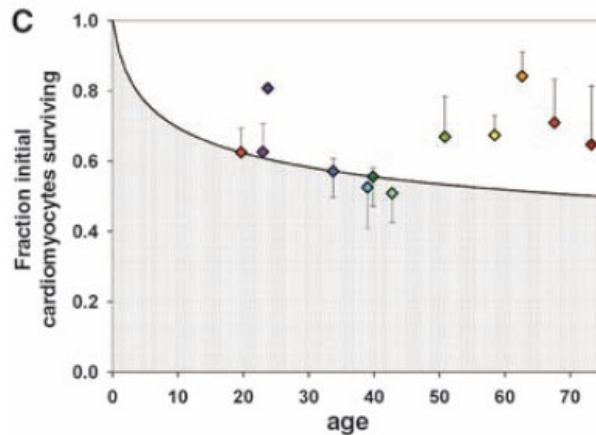


Fig. 1. Cell turnover in the heart. **(A)** Schematic figure demonstrating the strategy to establish cell age by ^{14}C dating. The black curve in all graphs shows the atmospheric concentrations of ^{14}C over the decades since 1930 [data from (14)]. The vertical bar indicates the date of birth of the individual. The measured ^{14}C concentration (1) is related to the atmospheric ^{14}C concentration by use of the established atmospheric ^{14}C bomb curve (2). The average birth date of the population can be inferred by determining where the data point intersects the x axis (3). ^{14}C concentrations in DNA of cells from the left ventricle myocardium in

individuals born after **(B)** or before **(C)** the nuclear bomb tests correspond to time points substantially after the time of birth, indicating postnatal cell turnover. The vertical bar indicates the date of birth of each individual, and the similarly colored dots represent the ^{14}C data for the same individual. For individuals born before the increase in ^{14}C concentrations, it is not possible to directly infer an age because the measured concentration can be a result of ^{14}C incorporation during the rising and/or falling part of the atmospheric curve, and thus the concentration is indicated by a dotted horizontal line.

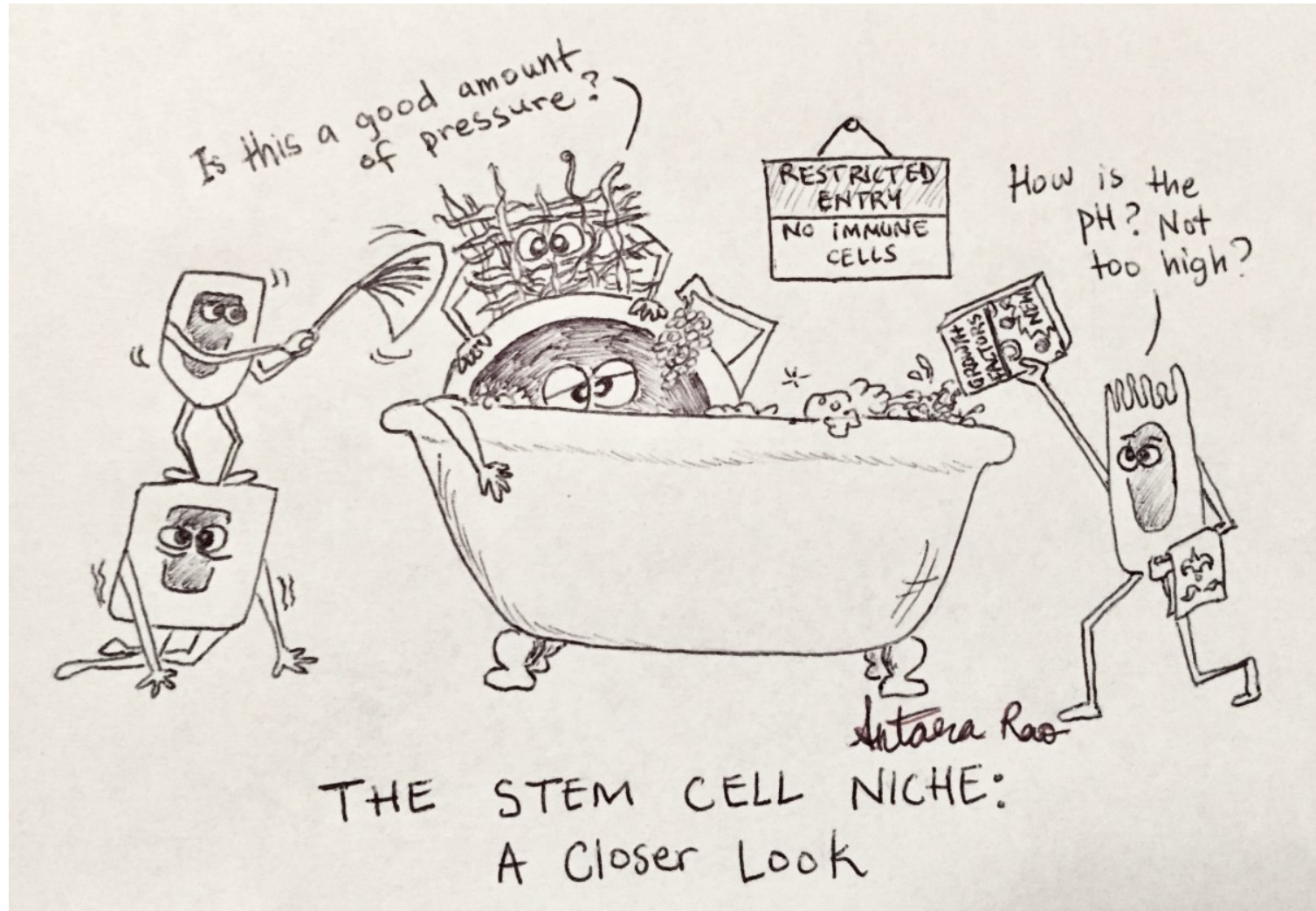


**Kde jsou tkáňově-specifické
kmenové buňky a jak
vypadají?**

Vlastnosti tkáňových kmenových buněk

- Kmenové buňky jednotlivých tkání a typů se vzájemně liší – co se týče např. schopnosti proliferovat nebo naopak zůstat zcela „inaktivní“ (quiescent)
- V biologii kmenových buněk mají zásadní význam dráhy kontrolující embryonální vývoj – např. Wnt, FGF, Hedgehog, Notch atd.
- Kmenové buňky zodpovědné za obměnu tkání v rámci homeostázy se mohou lišit od těch, které se aktivují v procesu regenerace
- Kmenové buňky jsou pod kontrolou svého mikroprostředí – tzv. niky kmenových buněk (stem cell niche)

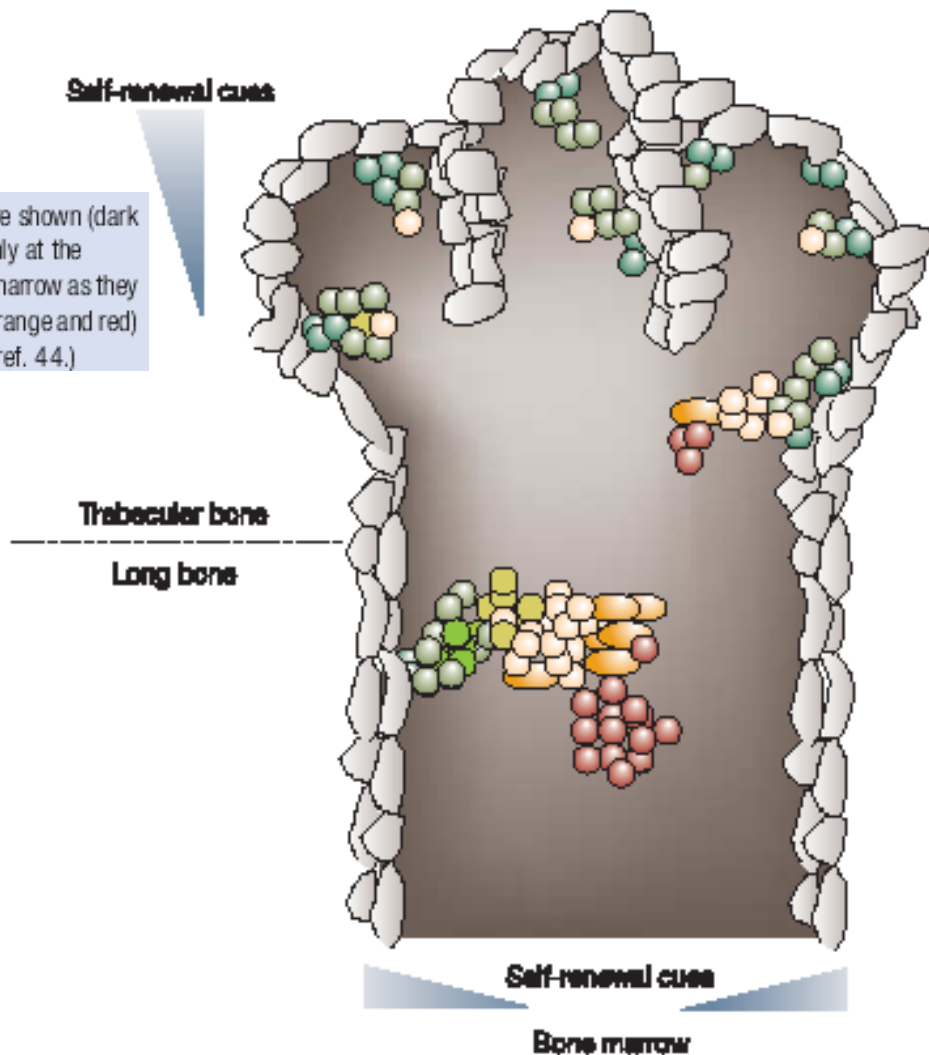
Nika kmenových buněk – stem cell niche



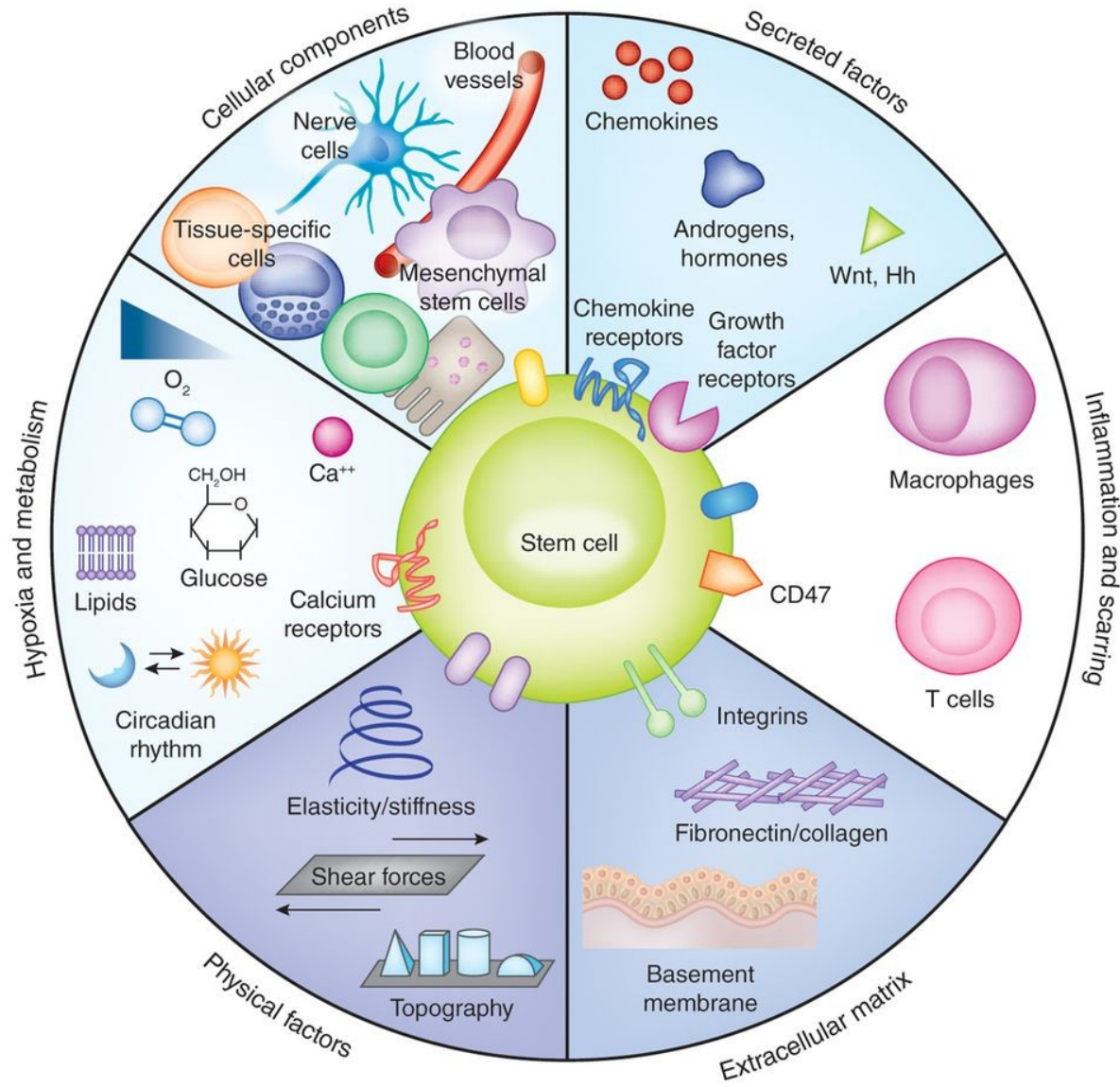
Prostředí kmenových buněk (stem cell niche)

kostní dřeň

Figure 5 Proposed model of HSC development in the niche. HSCs are shown (dark green) at the endosteal marrow adjacent to the bone's surface mainly at the trabecular bone, and are postulated to migrate inward in the central marrow as they differentiate (precursors in light green; differentiated cells in yellow, orange and red) away from a possible gradient of self-renewal cues. (Adapted from ref. 44.)



Komplexita „stem cell niche“

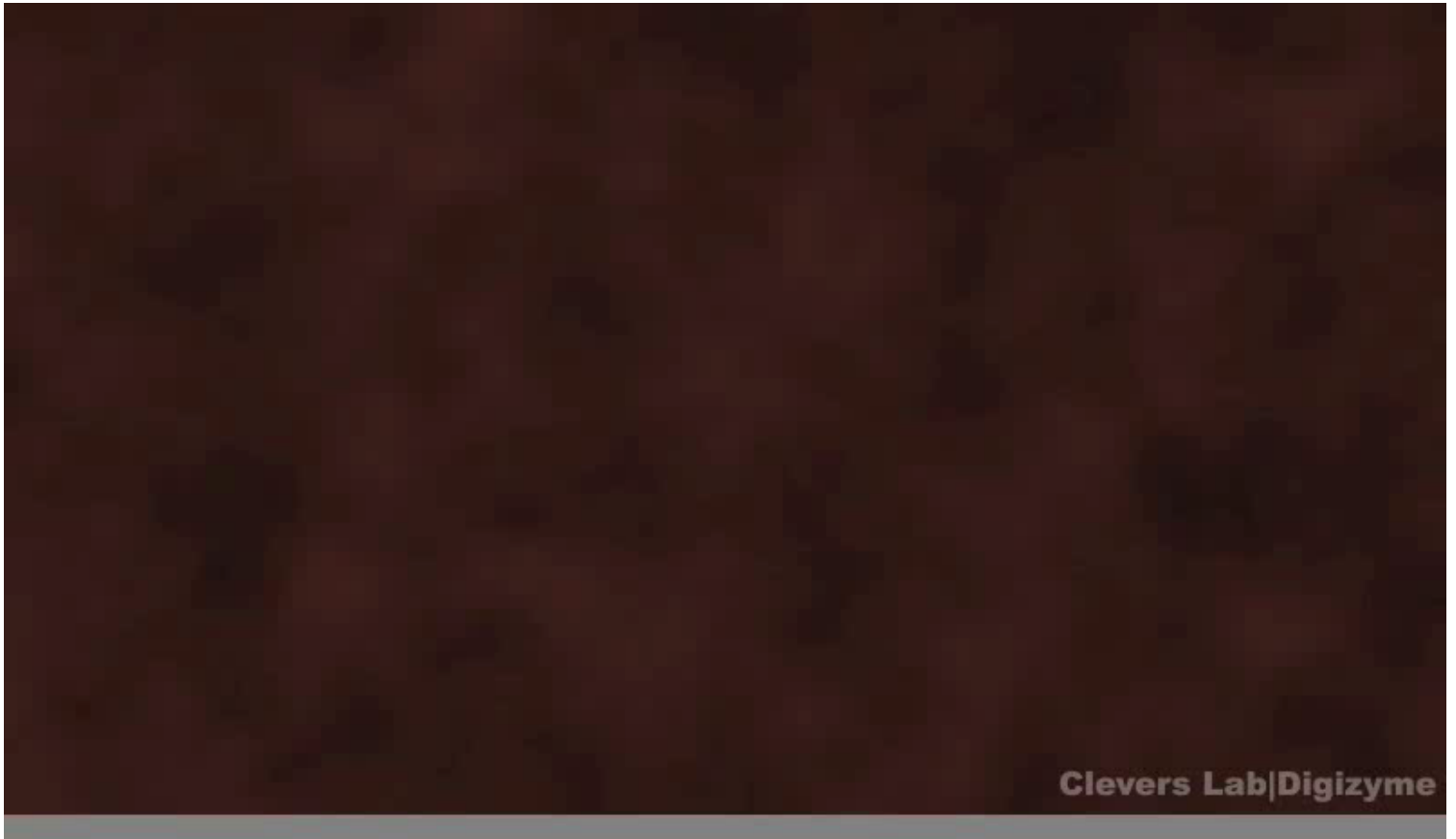


Epitel střeva jako modelový příklad funkce tkáňových buněk a hierarchické organizace tkání

- ▶ S využitím klíčových objevů prof. Hanse Cleverse (Utrecht) a jeho animací



Kmenové buňky střevního epitelu

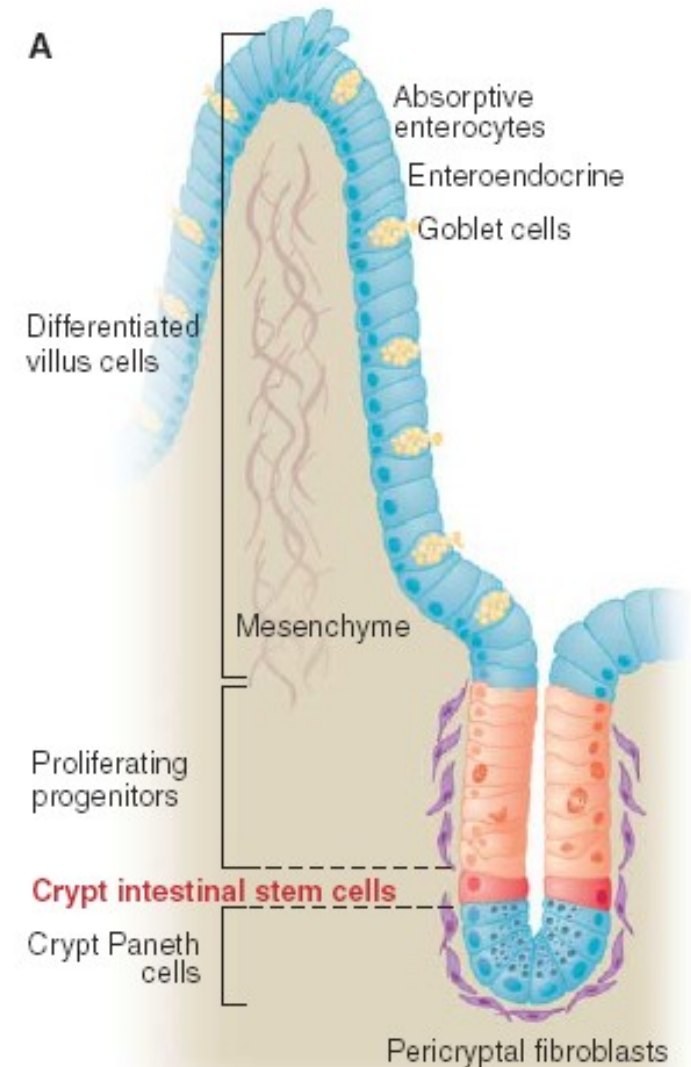


Kmenové buňky střeva (2006)

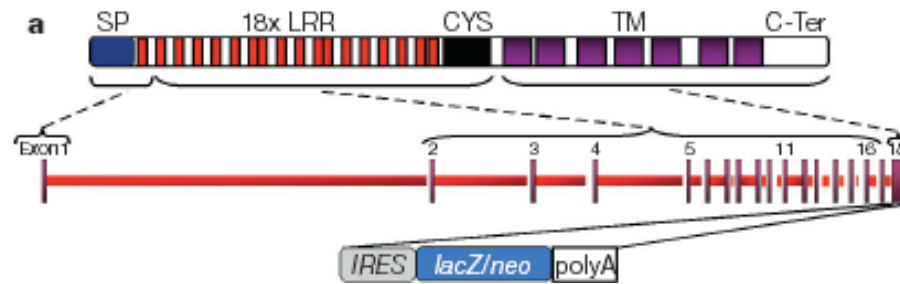
střevní epitel

2006: kmenové buňky definovány jako „label-retaining cells“

- tj. jako buňky, které se nedělí



Hon za dospělými kmenovými buňkami – Lgr5



střevní epitel – jak prokázat, že je buňka kmenová (Barker et al., Nature, October 2007)

A. Příprava transgenní myši č. 1 za účelem zjistit, kde je nový potenciální stem cell marker exprimován (in vivo expression profiling). Lgr5 je exprimován specificky v buňkách ve spodní části krypty.

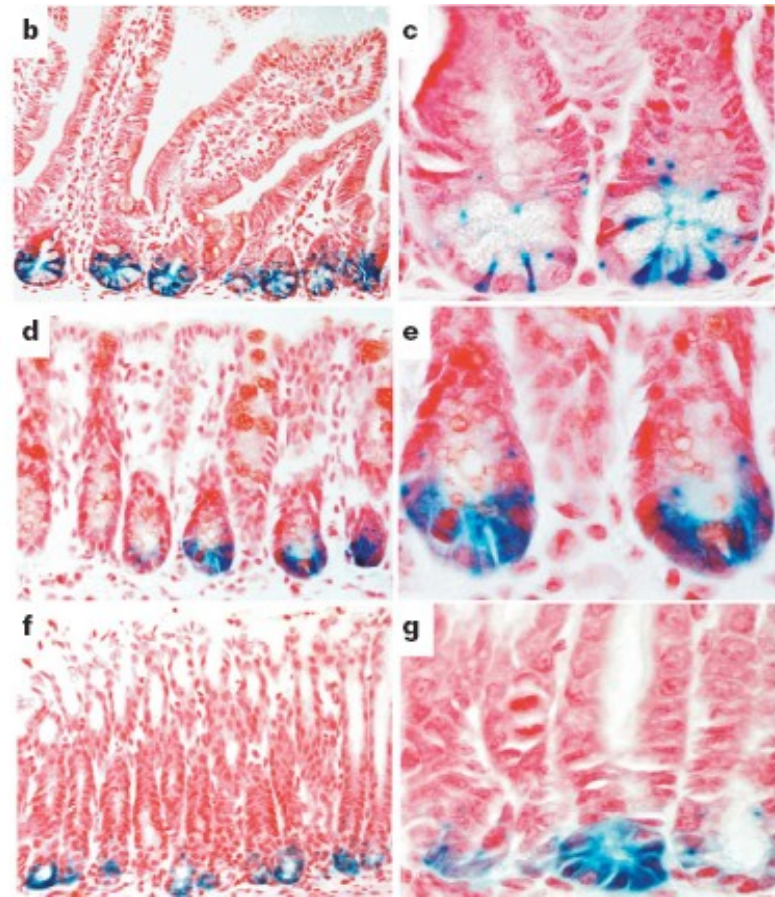
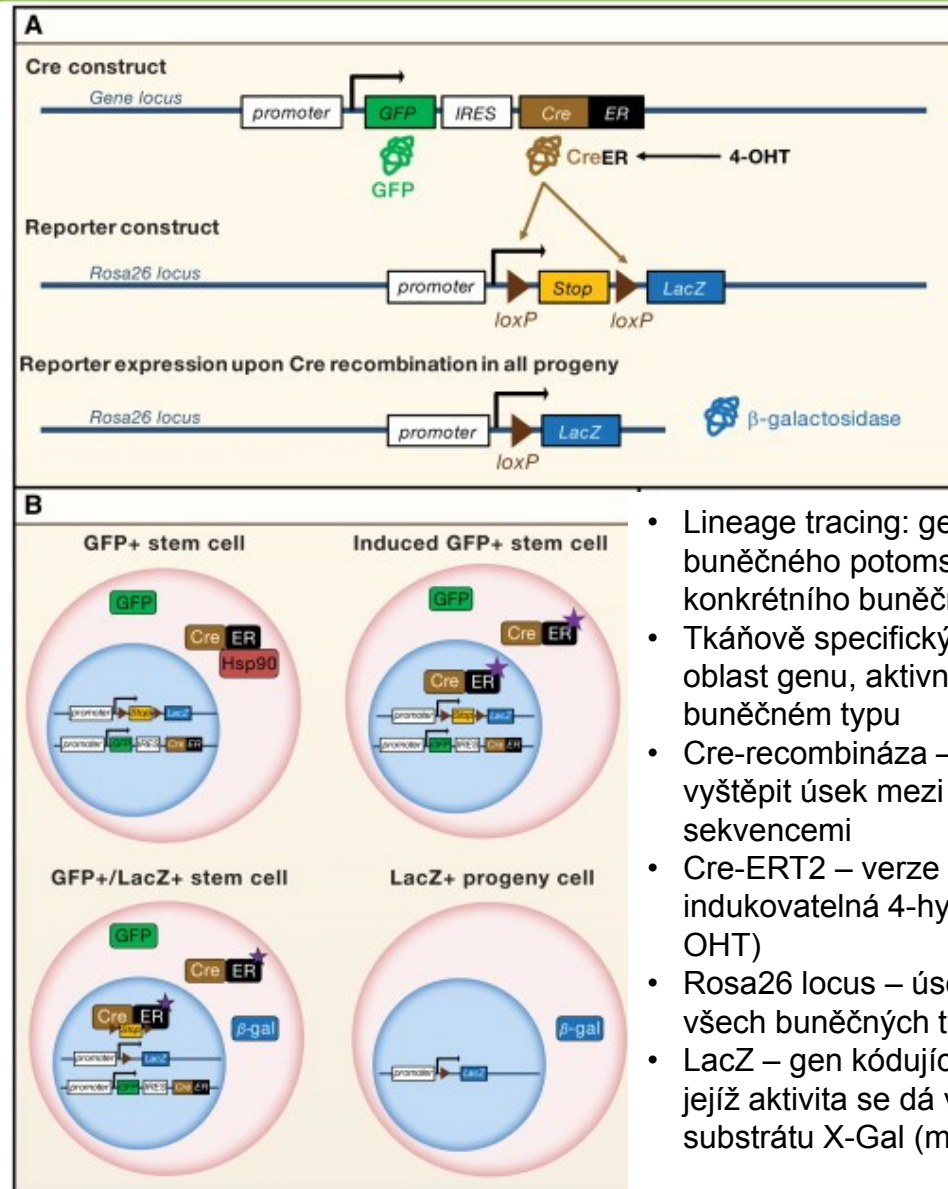


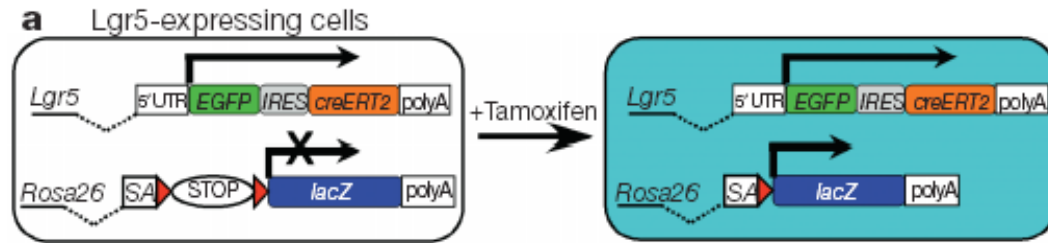
Figure 3 | Restricted expression of an *Lgr5-lacZ* reporter gene in adult mice. **a**, Generation of mice carrying *lacZ* integrated into the last exon of the *Lgr5* gene, removing all transmembrane (TM) regions of the encoded *Lgr5* protein. Neo, neomycin resistance cassette; SP, signal peptide; LRR, leucine-rich repeat region; C-Ter is carboxy terminus. **b–h**, Expression of *Lgr5-LacZ* (blue) in selected adult mouse tissues. **b, c**, In the small intestine, expression is restricted to six to eight slender cells intermingled with the Paneth cells at the crypt base. **d, e**, In the colon, expression is confined to a few cells located at the crypt base. **f, g**, Expression in the stomach is limited to the base of the glands.

Cre-Lox systém: Lineage tracing



- Lineage tracing: genetické označení buněčného potomstva (progeny) konkrétního buněčného typu
- Tkáňově specifický promotor – regulační oblast genu, aktivní pouze v konkrétním buněčném typu
- Cre-recombináza – enzym schopný vyštvěpit úsek mezi dvěma LoxP sekvencemi
- Cre-ERT2 – verze Cre-recombinázy indukovatelná 4-hydroxy-tamoxifenem (4-OHT)
- Rosa26 locus – úsek genomu, aktivní ve všech buněčných typech
- LacZ – gen kódující beta-galaktosidázu, jejíž aktivita se dá vizualizovat pomocí substrátu X-Gal (modré zbarvení)

Hon za dospělými kmenovými buňkami



střevní epitel – jak prokázat, že je buňka kmenová (Barker et al., Nature, October 2007)

B. Příprava transgenní myši 2, 3 a 4 za účelem zjistit, co všechno vzniká z *Lgr5*-pozitivních buněk (*Lgr5*+ lineage tracing). *Lgr5* pozitivní buňky dávají vzniknout všem částem buněčného epitelu.

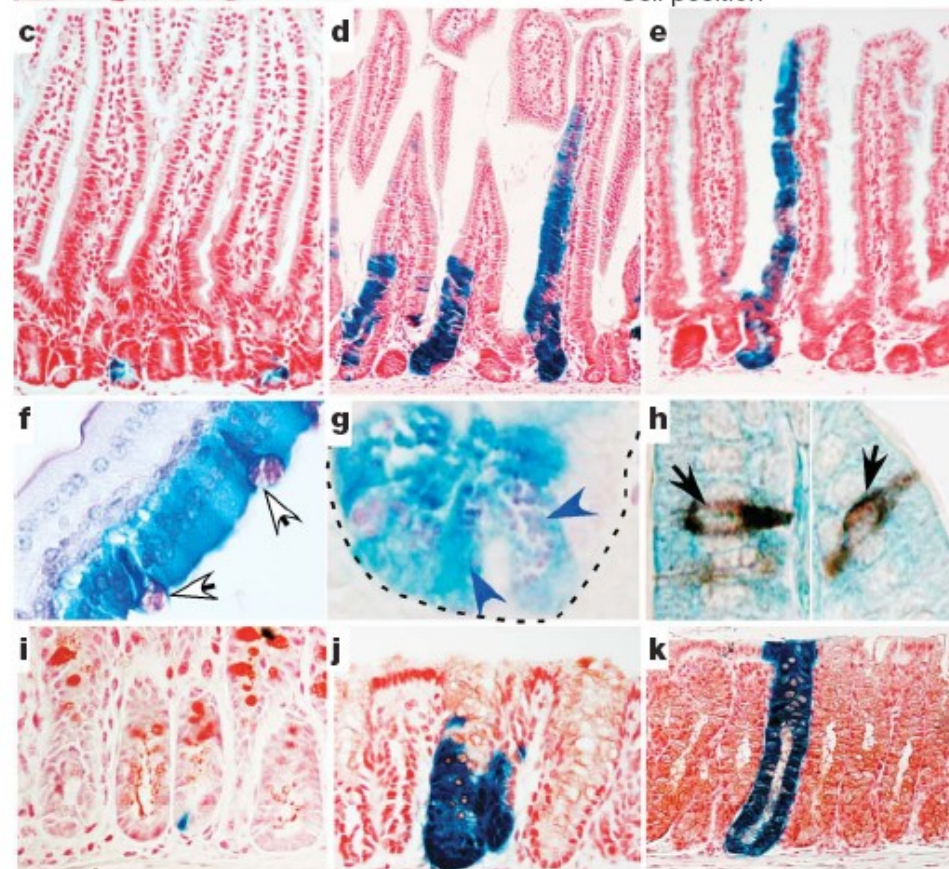
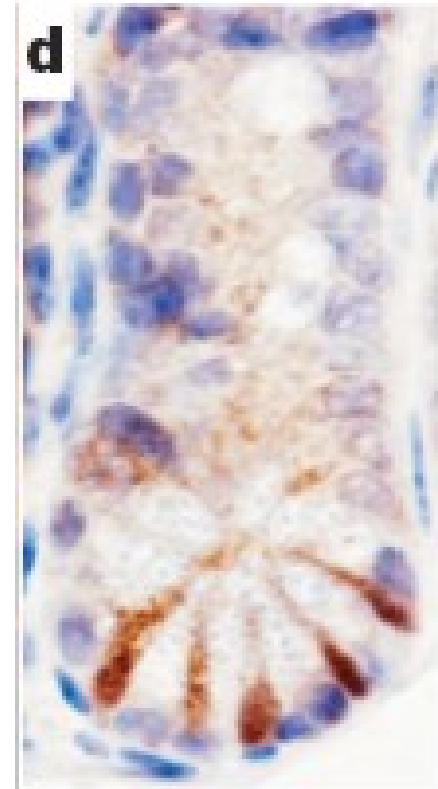
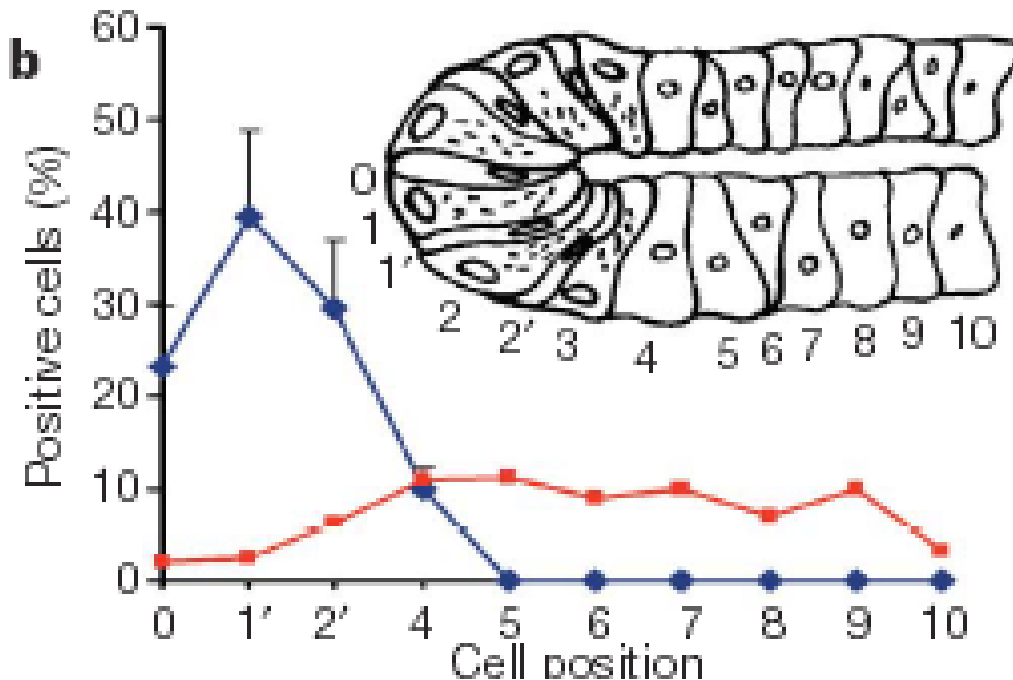


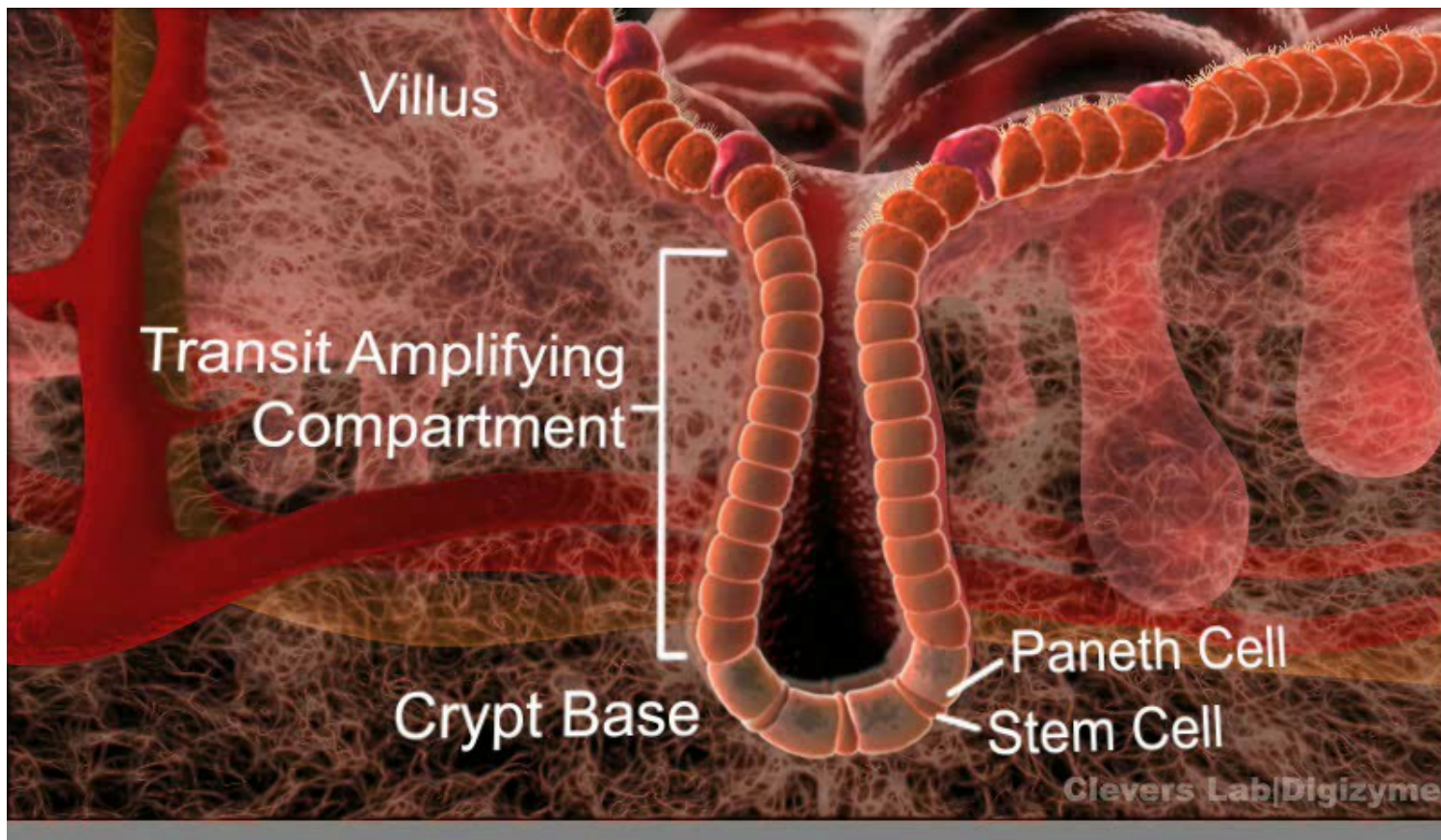
Figure 5 | Lineage tracing in the small intestine and colon. a, *Lgr5*-EGFP-IRES-creERT2 knock-in mouse crossed with *Rosa26*-lacZ reporter mice 12 h after tamoxifen injection. b, Frequency at which the blue cells appeared at carrying activated Cre. c–e, Histological analysis of LacZ activity in small intestine 1 day after induction (c), 5 days after induction (d) and 60 days after induction (e). f–h, Double-labelling of LacZ-stained intestine using PAS demonstrates the presence of goblet cells (f, white arrows) and Paneth cells (g, blue arrows) in induced blue clones. Double-labelling with synaptophysin demonstrates the presence of enteroendocrine cells within the induced blue clones (h, black arrows). i–k, Histological analysis of LacZ activity in colon 1 day after induction (i), 5 days after induction (j) and 60 days after induction (k).

Hon za dospělými kmenovými buňkami

střevní epitel –D. Závěr: Kmenové buňky epitelu tlustého i tenkého střeva jsou protáhlé, dříve nepovšimnuté buňky, v relativní pozici 1', 2' a 3' od spodu krypty.

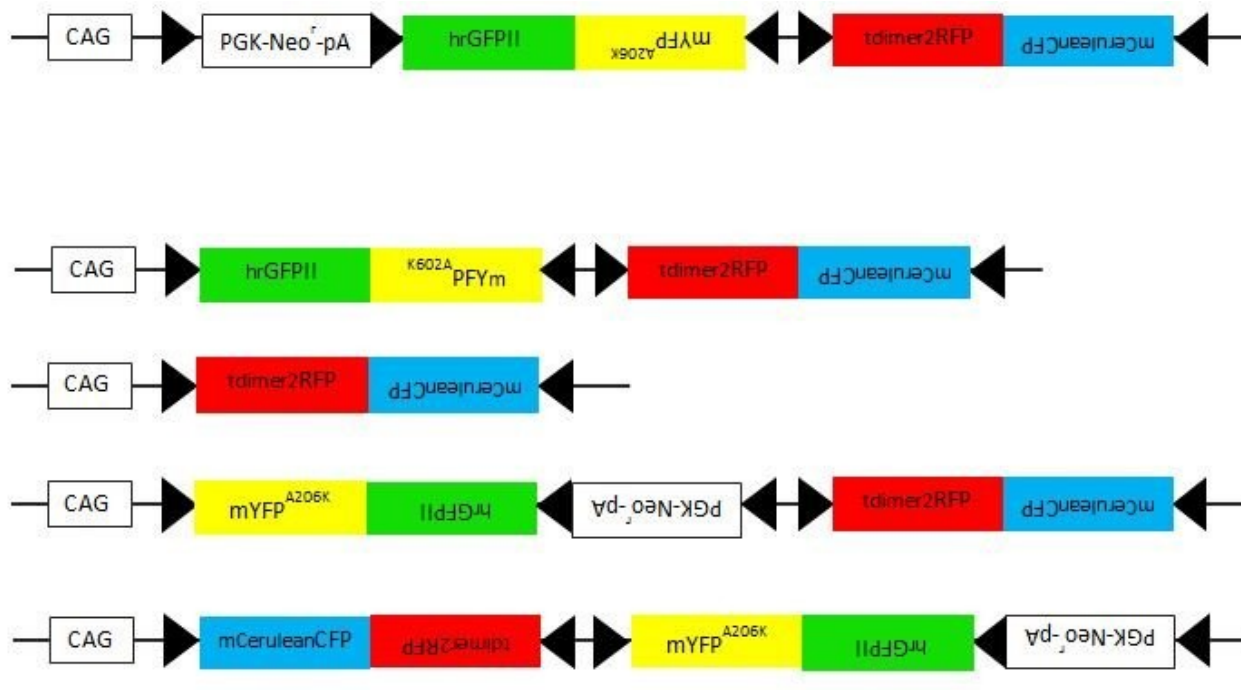


Fyziologie buň. systému



Jsou si kmenové buňky rovnocenné?

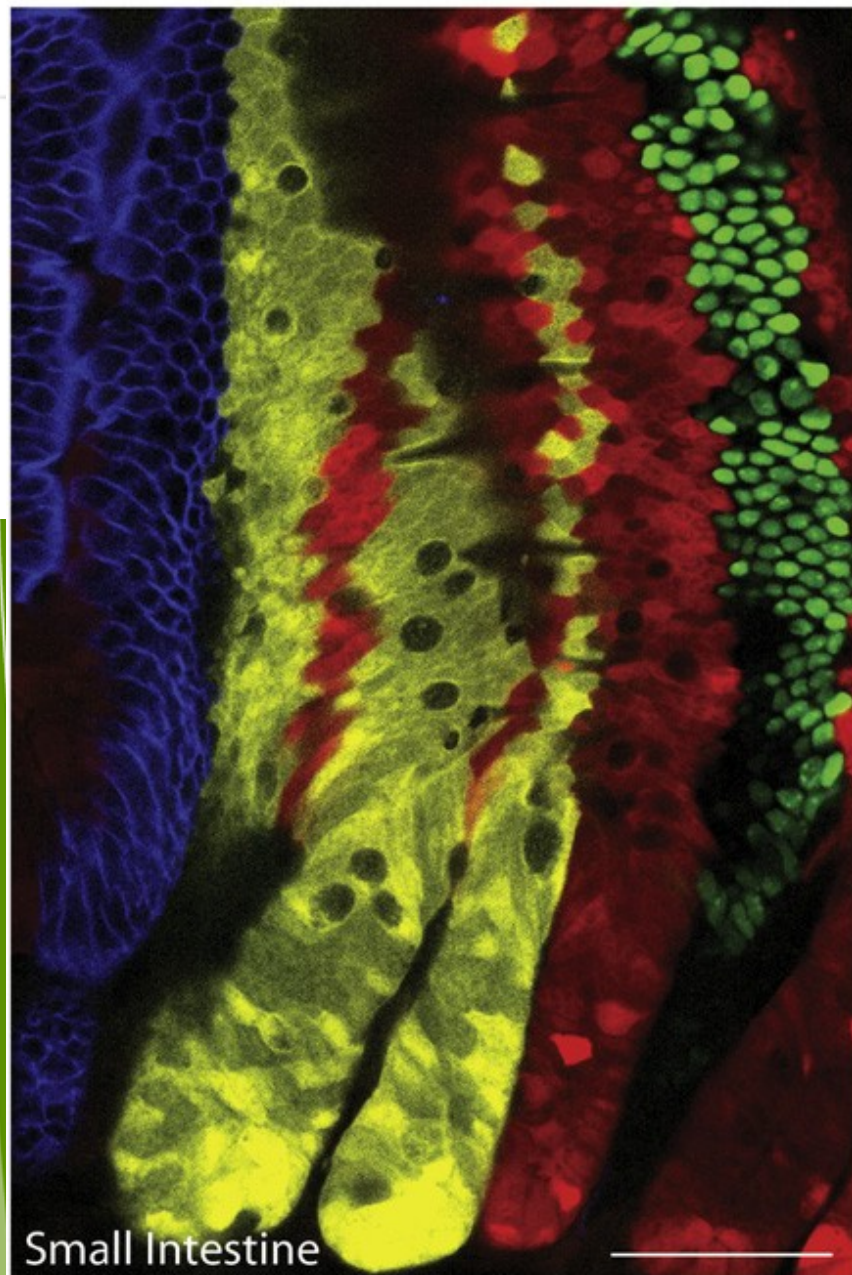
► Lineage tracing pomocí systému Confetti



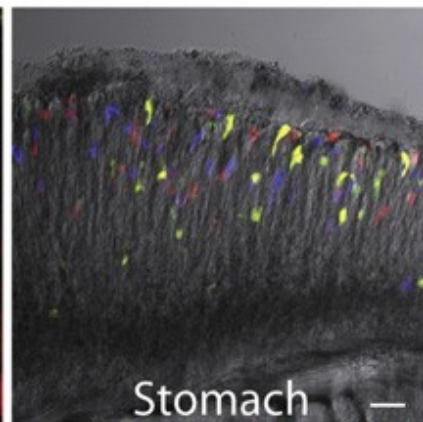
- Čtyři **LoxP** sekvence ohraničující geny pro čtyři fluorescenční proteiny **GFP**, **YFP**, **RFP** a **CFP**
- Cre-rekombinázy náhodně štěpí mezi dvěma **LoxP** místy
- Každá buňka a její potomstvo, ve které proběhne rekombinace se obarví **zeleně**, **žlutě**, **červeně** a **modře**

Rosa26 locus in Mouse, Chr6

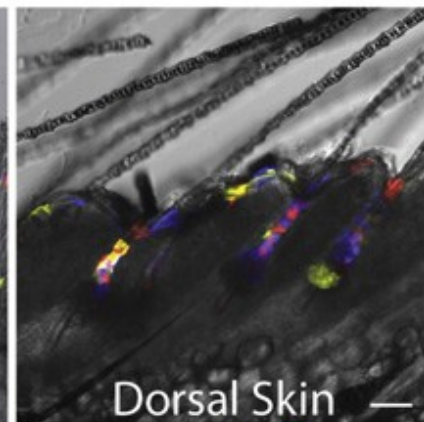
Cre recombination



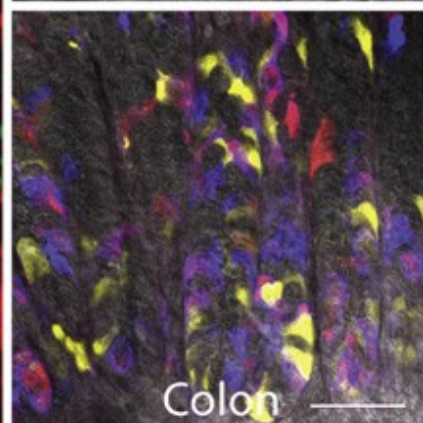
Small Intestine



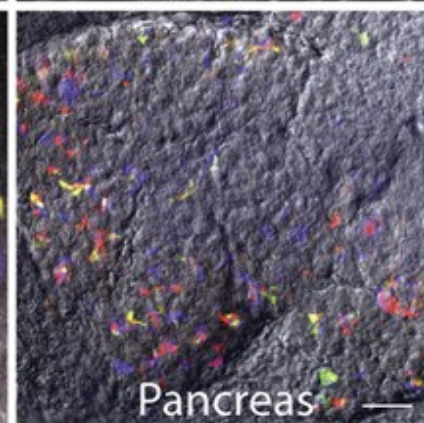
Stomach



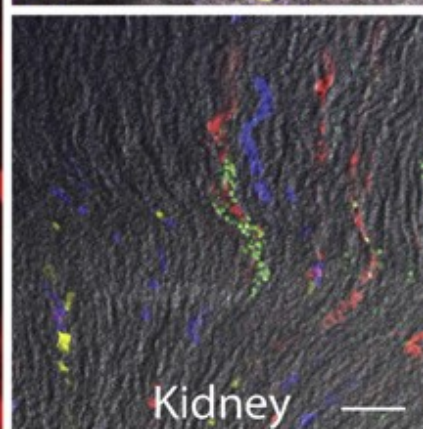
Dorsal Skin



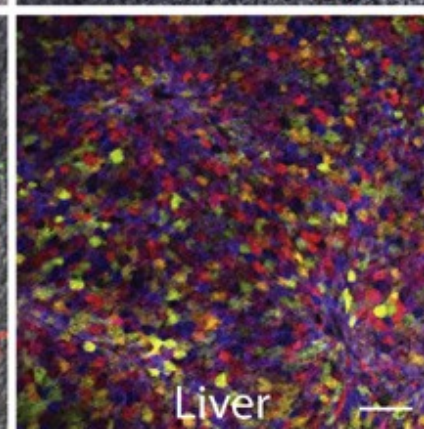
Colon



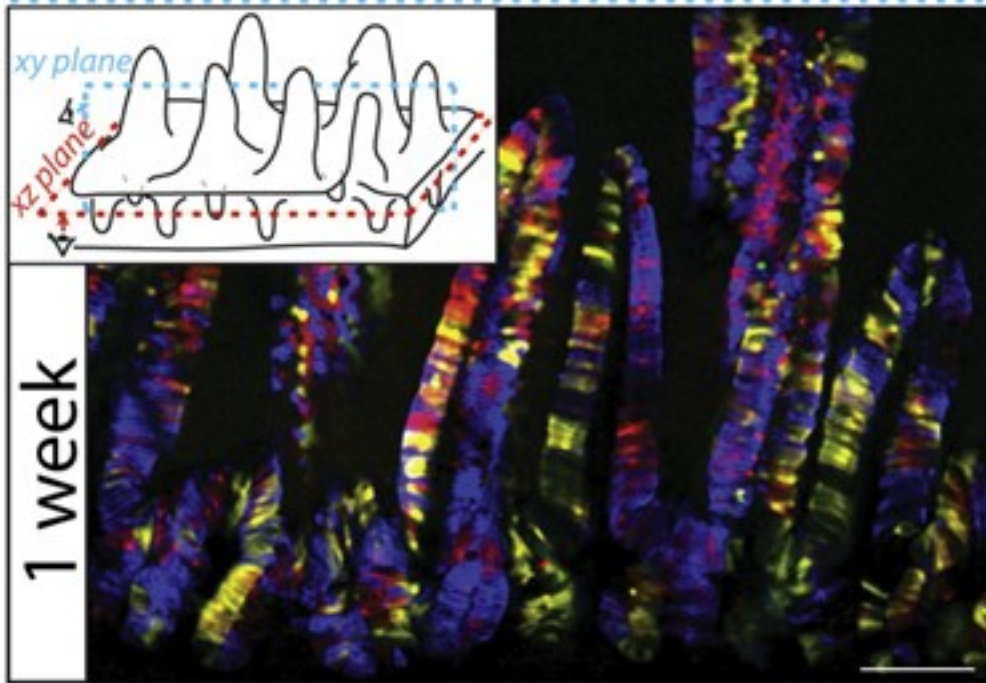
Pancreas



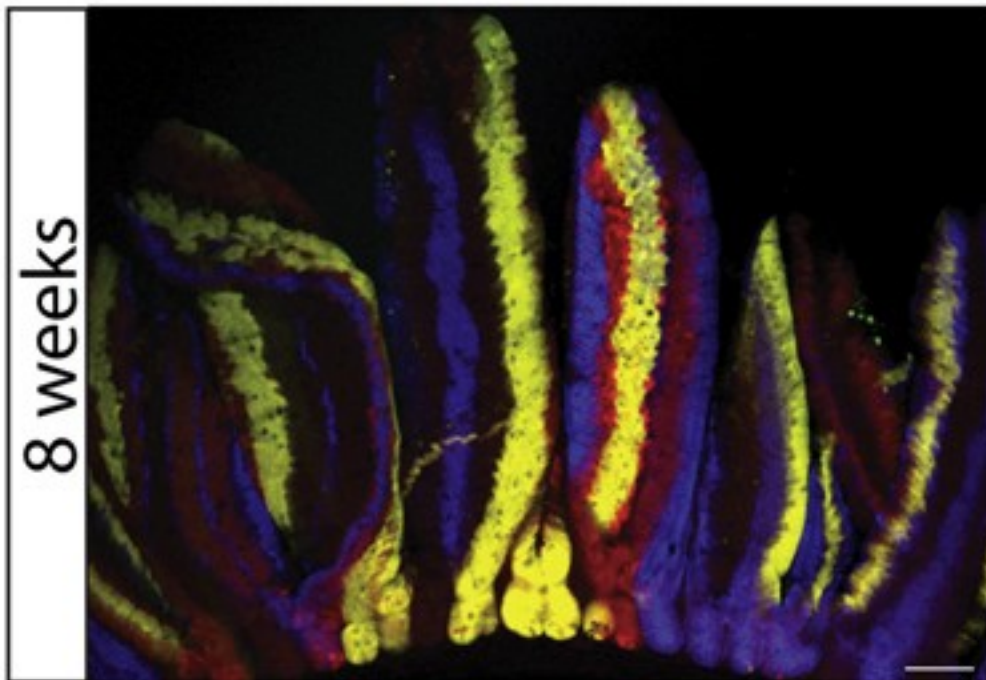
Kidney



Liver



1 week



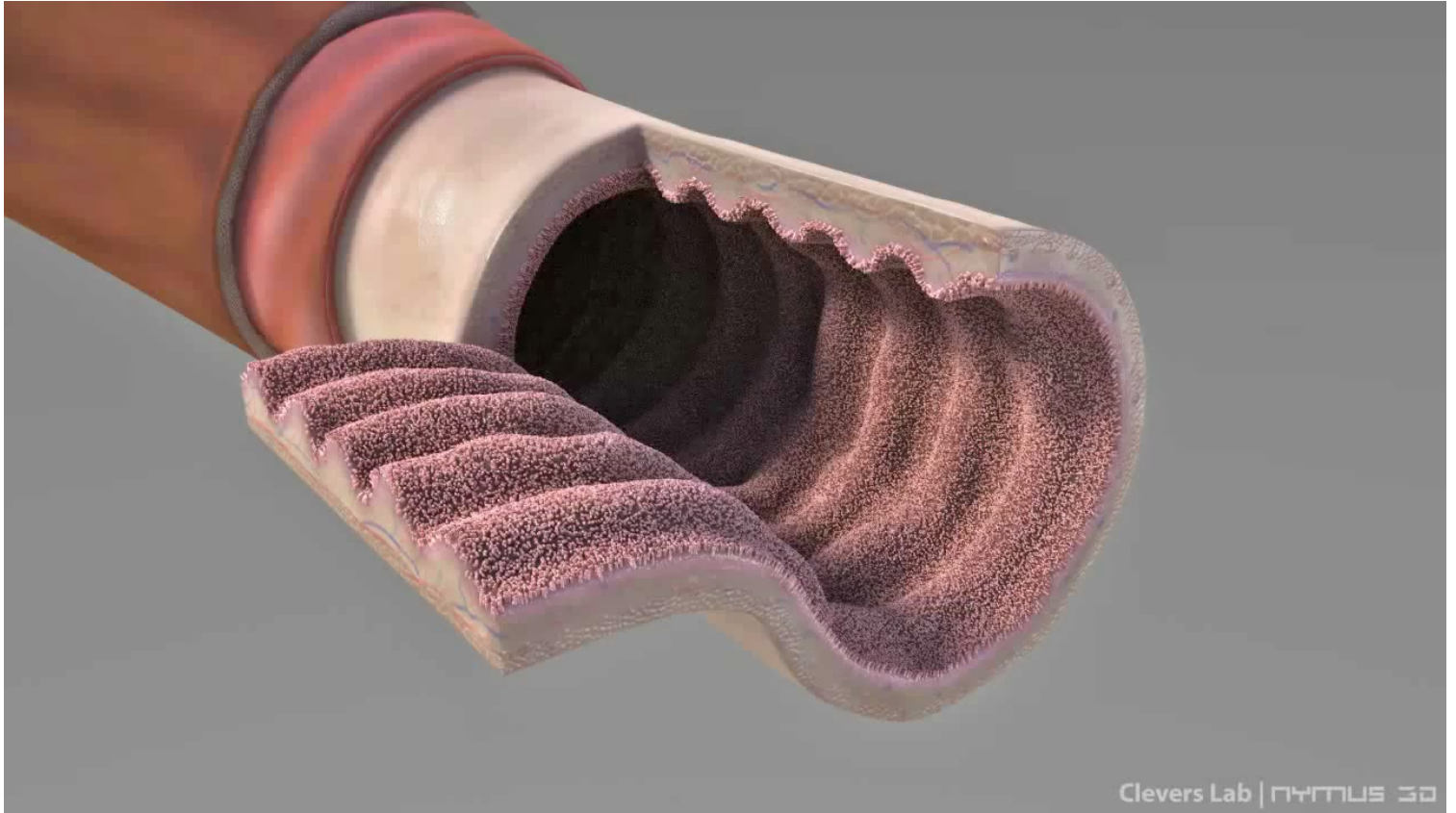
8 weeks

Cell

Intestinal Crypt Homeostasis Results from Neutral Competition between Symmetrically Dividing Lgr5 Stem Cells

Hugo J. Snippert,¹ Laurens G. van der Flier,¹ Toshiro Sato,¹ Johan H. van Es,¹ Maaïke van den Born,¹ Carla Kroon-Veenboer,¹ Nick Barker,¹ Allon M. Klein,^{2,3} Jacco van Rheenen,¹ Benjamin D. Simons,³ and Hans Clevers^{1,*}
¹Hubrecht Institute, KNAW and University Medical Center Utrecht, Uppsalalaan 8, 3584 CT Utrecht, The Netherlands
²Department of Systems Biology, Harvard Medical School, 200 Longwood Avenue, Boston, MA 02115, USA
³Department of Physics, Cavendish Laboratory, J.J. Thomson Avenue, Cambridge CB3 0HE, UK
 *Correspondence: h.clevers@hubrecht.eu
 DOI 10.1016/j.cell.2010.09.016

Stem cell competition - movie



Stem cell niche v epitelu střeva

LETTER

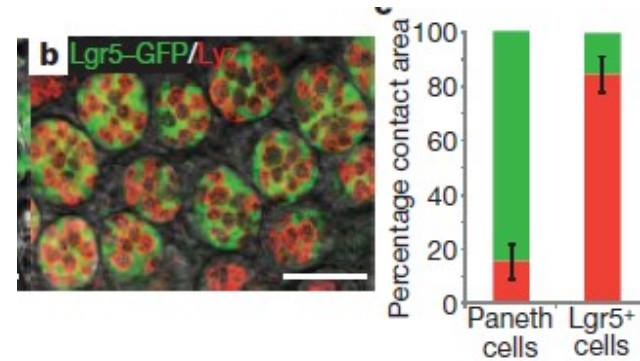
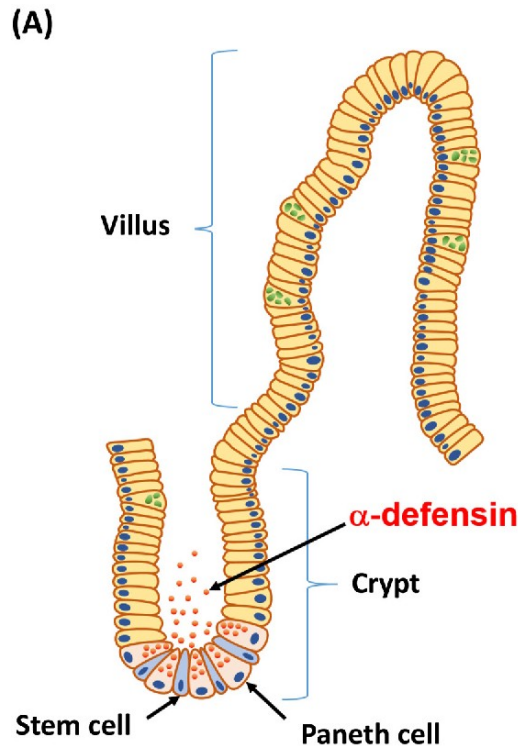
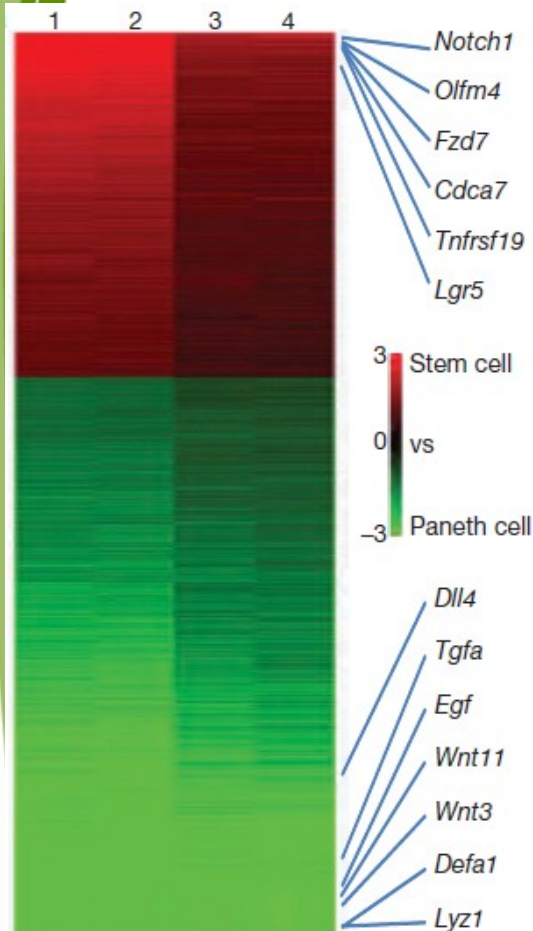
doi:10.1038/nature09637

Paneth cells constitute the niche for Lgr5 stem cells in intestinal crypts

Toshiro Sato¹, Johan H. van Es¹, Hugo J. Snippert¹, Daniel E. Stange¹, Robert G. Vries¹, Maaïke van den Born¹, Nick Barker¹, Noah F. Shroyer², Marc van de Wetering¹ & Hans Clevers¹

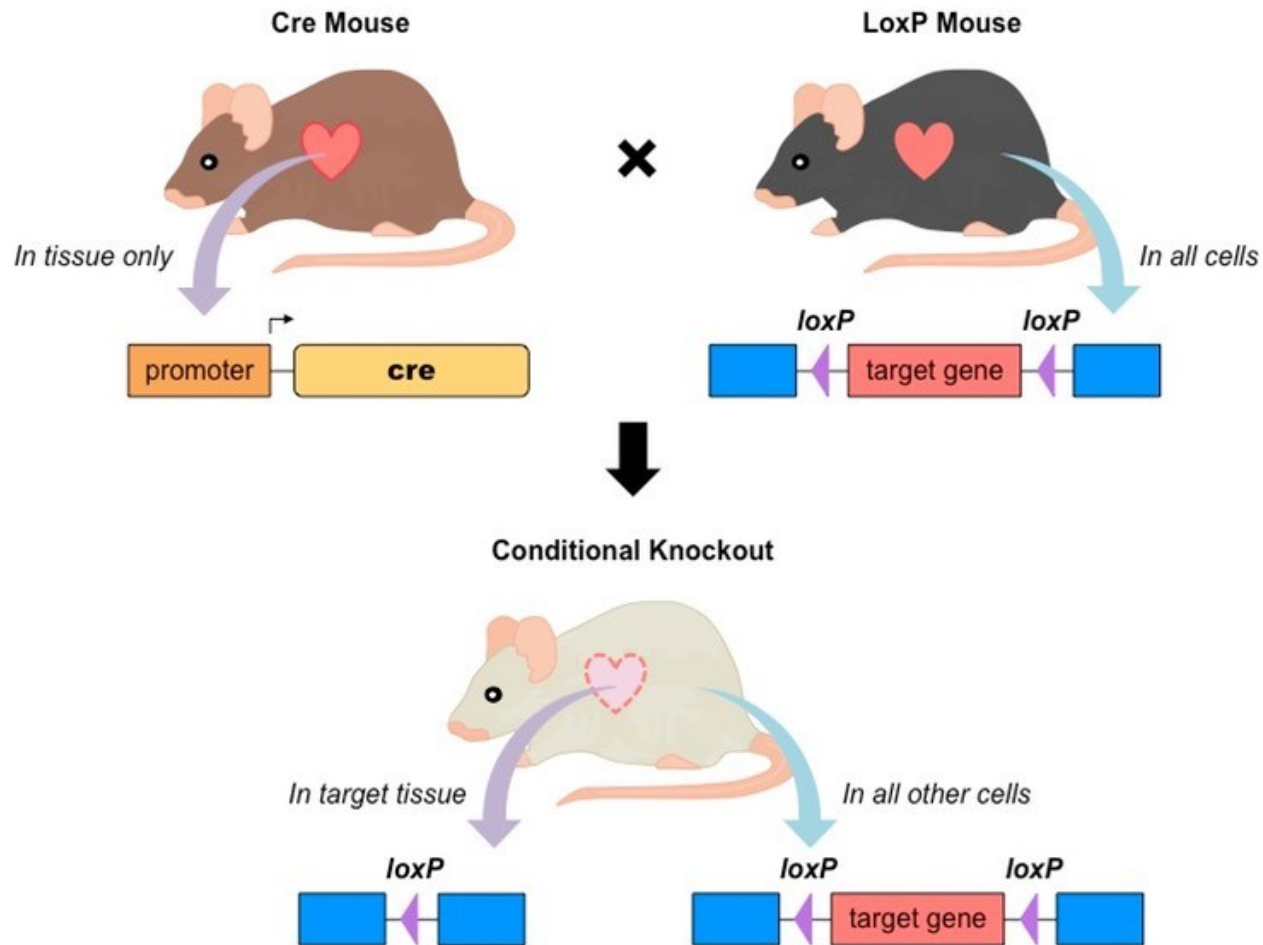
¹Recht Institute, KNAW and University Medical Center Utrecht, Uppsalalaan 8, 3584CT Utrecht, the Netherlands. ²Cincinnati Children's Hospital, Division of Gastroenterology, Medical Center, MLC 3, 3333 Burnet Avenue, Cincinnati, Ohio 45229, USA.

20 JANUARY 2011 | VOL 469 | NATURE | 415



Stem cell niche v epitelu střeva

Kondicionální/tkáňově specifický knockout genu



Stem cell niche v epitelu střeva

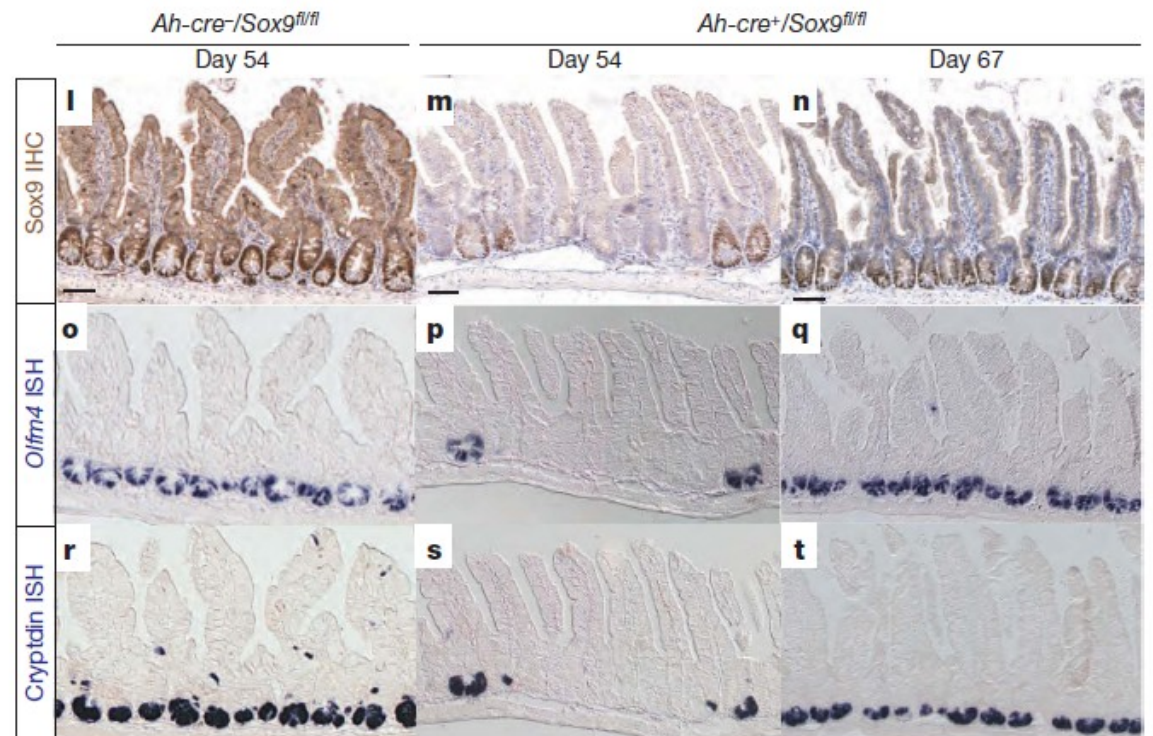
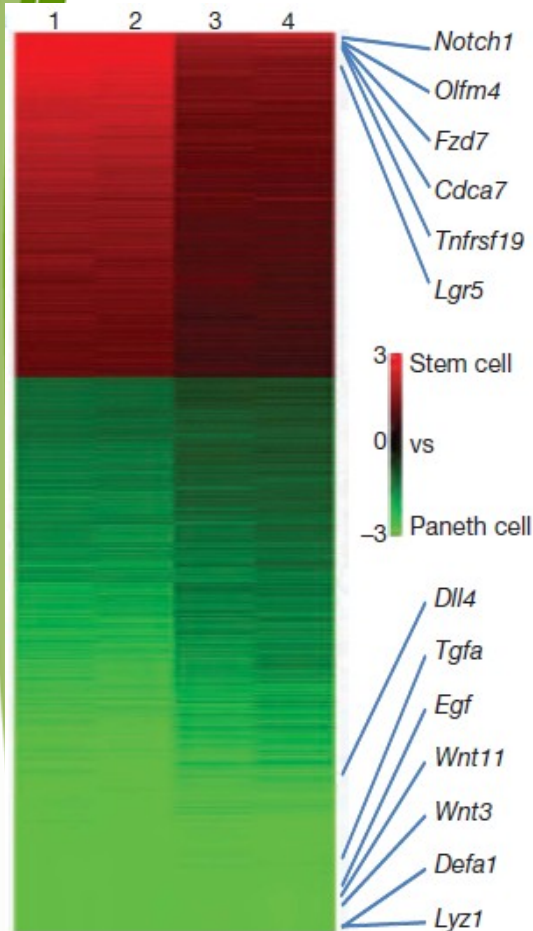
LETTER

doi:10.1038/nature09637

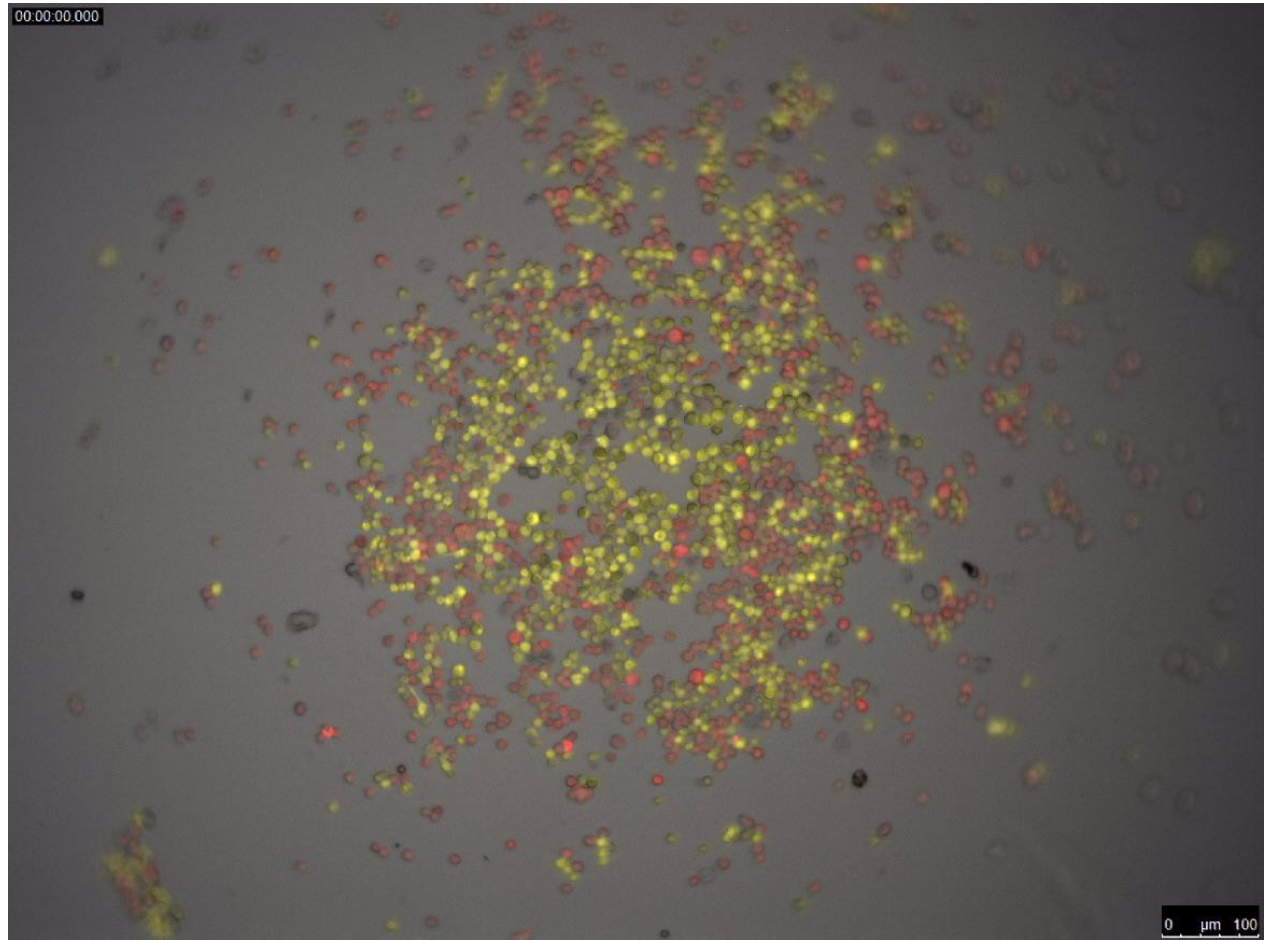
Paneth cells constitute the niche for Lgr5 stem cells in intestinal crypts

Toshiro Sato¹, Johan H. van Es¹, Hugo J. Snippert¹, Daniel E. Stange¹, Robert G. Vries¹, Maaïke van den Born¹, Nick Barker¹, Noah F. Shroyer², Marc van de Wetering¹ & Hans Clevers¹

¹brecht Institute, KNAW and University Medical Center Utrecht, Uppsalalaan 8, 3584CT Utrecht, the Netherlands. ²Cincinnati Children's Hospital, Division of Gastroenterology, Medical Center, ML 0, 3333 Burnet Avenue, Cincinnati, Ohio 45229, USA.



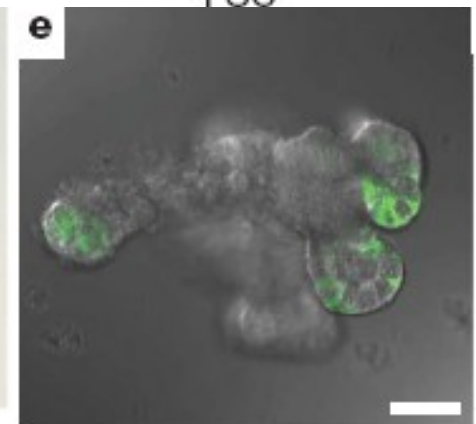
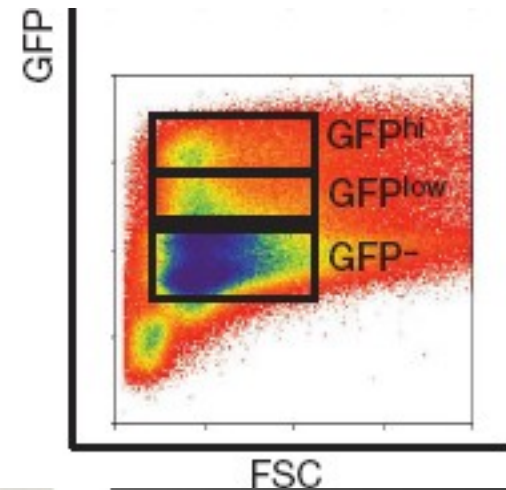
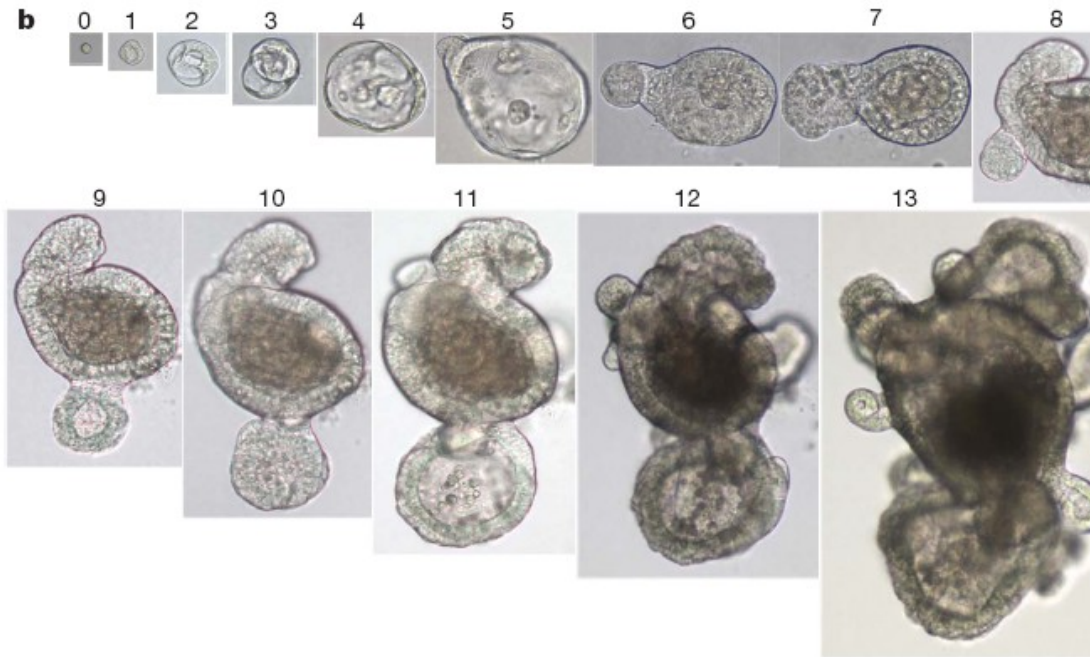
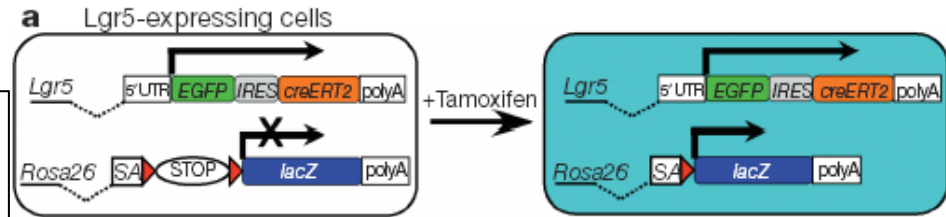
Panetovy buňky jako „niche“ kmenových buněk střeva



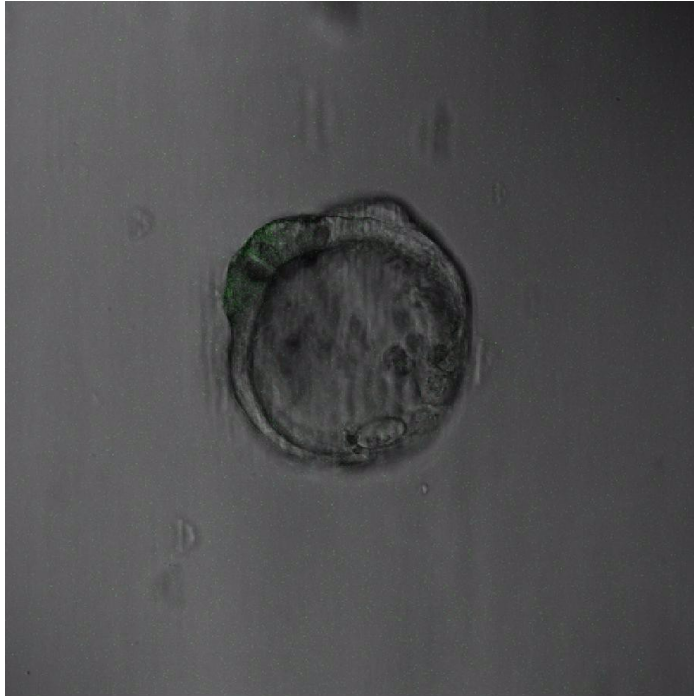
Organoidy

Organoidy

C. *Lgr5* pozitivní buňky in vitro dávají vzniknout kompletní villus-crypt struktuře in vitro (Doposud se to s žádnými jinými buňkami nepodařilo)



Organoidy



Organoid je miniaturizovaná a zjednodušená verze orgánu vyráběná in vitro ve třech rozměrech, která navíc vykazuje realistickou mikroanatomii. Organoid je odvozen z jedné nebo několika buněk z tkáně, embryonálních kmenových buněk nebo indukovaných pluripotentních kmenových buněk, které se mohou samoorganizovat ve třídídimenzionální kultuře díky schopnosti sebeobnovy a diferenciaci. Technika růstu organoidů se od počátku roku 2010 rychle zlepšila a byla jmenována The Scientist jako jeden z největších vědeckých pokroků v roce 2013. (wikipedie)

Organoidy

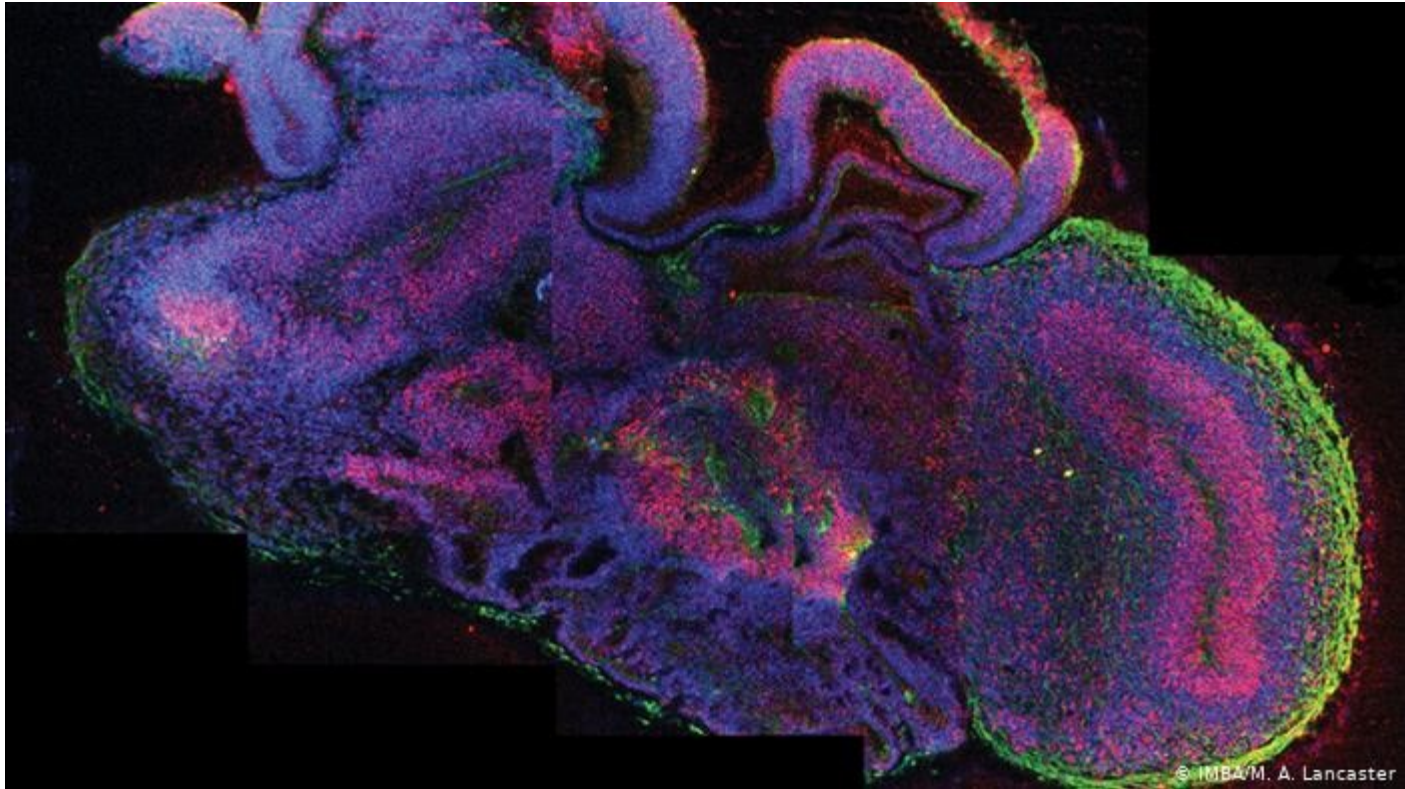
Table 2 Organoid models from various organs and ESCs/iPSCs

Tissue	Source	Organoid morphology	Cell types in organoid	Downstream applications tested	Types of human diseases modelled
Lingual	Mouse lingual stem cells	Spherical and budding organoids	-Stratum corneum -Keratin 5/14+ stem/progenitor cells -Granular cells of intermediate epithelial origin	-Tamoxifen inductions -Lineage tracing -Engraftment studies	Lingual carcinoma
Taste bud	Murine circumvallate tissue	Spherical and budding organoids	-Lgr5+ stem cells -Lgr6+ stem/progenitor cells -UEA/K8+ intragemmal taste bud cells -Gustducin-expressing, T1R3-expressing mature taste receptor cells -Sox9+ proliferative cells in budding regions	-Functional assays -Gene expression analysis -Cell cycle analysis	-
Salivary gland	Primary mouse cells	-Ductal branching organoids -Lobular spherical organoids	-CD24 ^{hi} /CD29 ^{hi} stem cells -Cytokeratin 7/18+ duct cells. -Aquaporin5-expressing acinar cells	-Gene expression analysis -Transplantation studies	Hyposalivation
Oesophagus	Mouse/human adult oesophageal tissue	-Spherical multilayered organoids -Human Barrett's oesophagus organoids: budding morphology	-CK14+, p63+ small basal cells in the outer layer, large basal cells in the middle layer, and CK13+ cells in the central keratinized layer -Integrin α_6/β_4^{low} differentiated and integrin α_6/β_4^{hi} stem cells -Barrett's oesophageal organoids express goblet cells following differentiation.	-Tamoxifen inductions -Gene expression analysis	Barrett's oesophagus
Stomach	-Mouse/human adult tissue -Mouse/human ESCs -Human iPSCs	-Pylorus and corpus: spherical organoids -FGF10-driven budding events in pyloric organoids	-Pylorus: Lgr5+ stem cells, mucous neck cells, pit cells, enteroendocrine cells -Corpus: chief cells, mucous neck cells, pit cells	-Microinjection and infection model for <i>H. pylori</i> -Transcriptome profiling -Co-culture with mesenchymal cells -Adeno/retroviral transfections	- <i>H. pylori</i> infection -Cancer
Intestine	-Adult tissue -Mouse/human ESCs -Human iPSCs	-Normal tissue: branching organoids -Diseased tissue: cystic and other morphologies	-Crypt-like domain contains Lgr5+ stem cells and paneth cells -Villus-like domain harbours villin+ cells -Enteroendocrine and goblet cells scattered throughout organoid	-Transplantation studies -CRISPR/Cas9 gene editing -Cancer mutations -Transcriptome profiling	-Cancer -Cystic fibrosis -Infection model for viral and bacterial infection
Colon	-Adult tissue -Mouse/human iPSCs	-Normal tissue: budding organoids -Diseased tissue: cystic morphologies	-Lgr5+ stem cells -Enteroendocrine cells -Goblet cells -Enterocytes -Lgr5+ stem cells and bile duct cells -Hepatocytes observed after inhibition of Notch	-Transplantation studies -Transcriptome profiling -Biobank	-IBD -Cancer

Organoidy

Liver	<ul style="list-style-type: none"> -Mouse adult tissue -Human iPSCs 	<ul style="list-style-type: none"> -Mouse organoids: spherical -Human organoids: cystic 	<p>& TGF-β pathways</p> <ul style="list-style-type: none"> -Human organoids contain Lgr5⁺ stem cells, ductal cells and hepatocytes -Cholangiocyte organoids express differentiation markers such as apical sodium-dependent bile acid transporter, secretin receptor, cilia and CFTR. 	<ul style="list-style-type: none"> -Transplantation studies -Transcriptome profiling -Adenoviral transduction -Whole-genome sequencing -CFTR functional assays 	<ul style="list-style-type: none"> -Alagille syndrome -Cystic fibrosis
Pancreas	<ul style="list-style-type: none"> Mouse/human adult tissue 	<ul style="list-style-type: none"> -E10.5 tissue: branching organoids -Adult tissue: budding organoids 	<ul style="list-style-type: none"> -Ductal organoids contain Lgr5⁺ stem cells -Organoids from E10.5 murine pancreas can be differentiated into exocrine and endocrine cells 	<ul style="list-style-type: none"> -Engraftment studies -Lineage tracing -Adenoviral transduction -Transcriptome profiling 	<ul style="list-style-type: none"> Cancer
Prostate	<ul style="list-style-type: none"> Mouse/human adult tissue 	<ul style="list-style-type: none"> -Normal tissue: spherical -Diseased tissue: branching similar to morphology of cancerous organoids 	<ul style="list-style-type: none"> -Cytokeratin 5/p63⁺ basal cells -Cytokeratin 8⁺ luminal cells. Lgr4/Lgr5⁺ cells -Uniform proximal Sox2 and distal Sox9 expression 	<ul style="list-style-type: none"> -Tamoxifen inductions -Lentiviral infections 	<ul style="list-style-type: none"> Cancer
Lung	<ul style="list-style-type: none"> -Mouse foetal pulmonary cells -Human ESCs/iPSCs 	<ul style="list-style-type: none"> Spherical organoids 	<ul style="list-style-type: none"> -Proximal-like domains included basal, ciliated and club cells that were surrounded by smooth-muscle actin -Outer layer recapitulates retinal pigment -Invaginated layer resembles retinal optic cup containing photoreceptors, ganglion cells, bipolar cells and Muller glia 	<ul style="list-style-type: none"> -Transplantation studies -Cancer mutations -RNA sequencing 	<ul style="list-style-type: none"> Cystic fibrosis
Retina	<ul style="list-style-type: none"> Mouse ESCs 	<ul style="list-style-type: none"> Spherical organoids 	<ul style="list-style-type: none"> -Functional prosensory vesicles -Otic vesicles also generate functional inner-ear hair cells 	<ul style="list-style-type: none"> - 	<ul style="list-style-type: none"> -
Inner ear	<ul style="list-style-type: none"> Mouse ESCs 	<ul style="list-style-type: none"> Budding organoids 	<ul style="list-style-type: none"> -Early-stage organoids contain continuous neuroepithelia -Cerebral cortical regions contain outer radial glia and cerebral cortical neurons 	<ul style="list-style-type: none"> - 	<ul style="list-style-type: none"> -
Brain	<ul style="list-style-type: none"> -Mouse/human ESCs -Human iPSCs -Patient skin fibroblasts 	<ul style="list-style-type: none"> -Early-stage spherical organoids -Later-stage budding organoids -Early-stage spherical organoids 	<ul style="list-style-type: none"> -Early-stage organoids contain continuous neuroepithelia -Cerebral cortical regions contain outer radial glia and cerebral cortical neurons 	<ul style="list-style-type: none"> -Transfection -Transcriptome profiling -Electrical excitation 	<ul style="list-style-type: none"> -Autism -Microcephaly
Kidney	<ul style="list-style-type: none"> Human iPSCs 	<ul style="list-style-type: none"> -Early-stage spherical organoids -Differentiated stages have budding morphology 	<ul style="list-style-type: none"> Differentiated organoids exhibit segmentation as ducts, tubules and glomeruli 	<ul style="list-style-type: none"> Toxicity screening in response to cisplatin 	<ul style="list-style-type: none"> -

Mozkové organoidy - minibrains



Lancaster MA, Renner M, Martin CA, Wenzel D, Bicknell LS, Hurles ME, Homfray T, Penninger JM, Jackson AP, Knoblich JA (September 2013). ["Cerebral organoids model human brain development and microcephaly"](#). *Nature*. **501** (7467): 373–9.

Využití organoidů pro buněčné terapie poruch funkce střeva – např. cystická fibroza

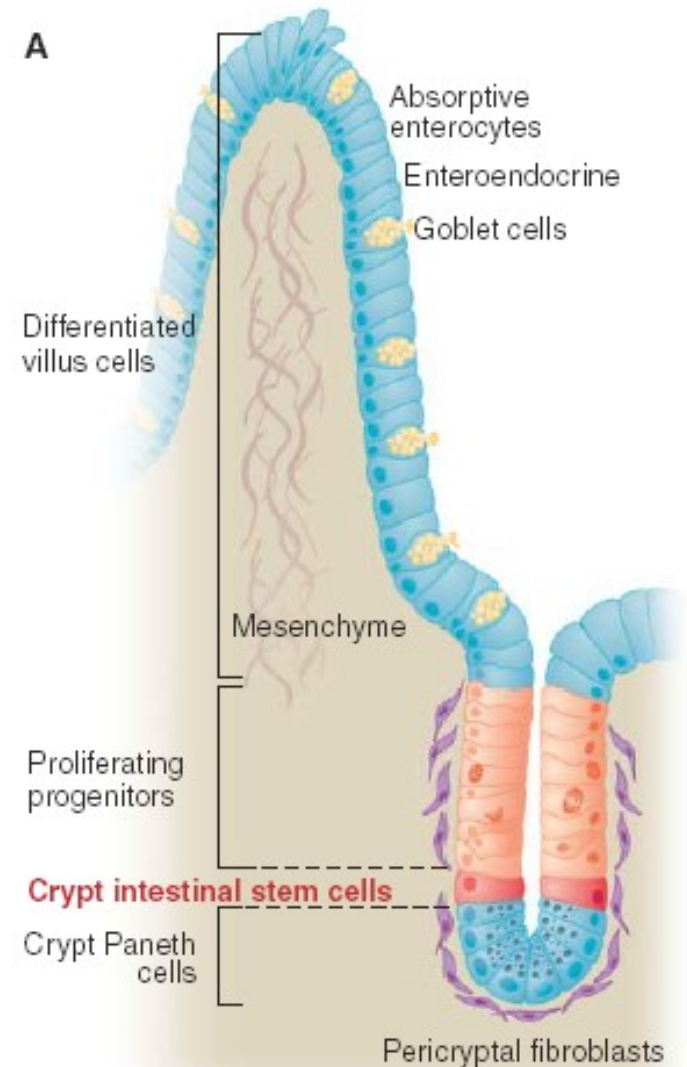


Kmenové buňky střeva (2006)

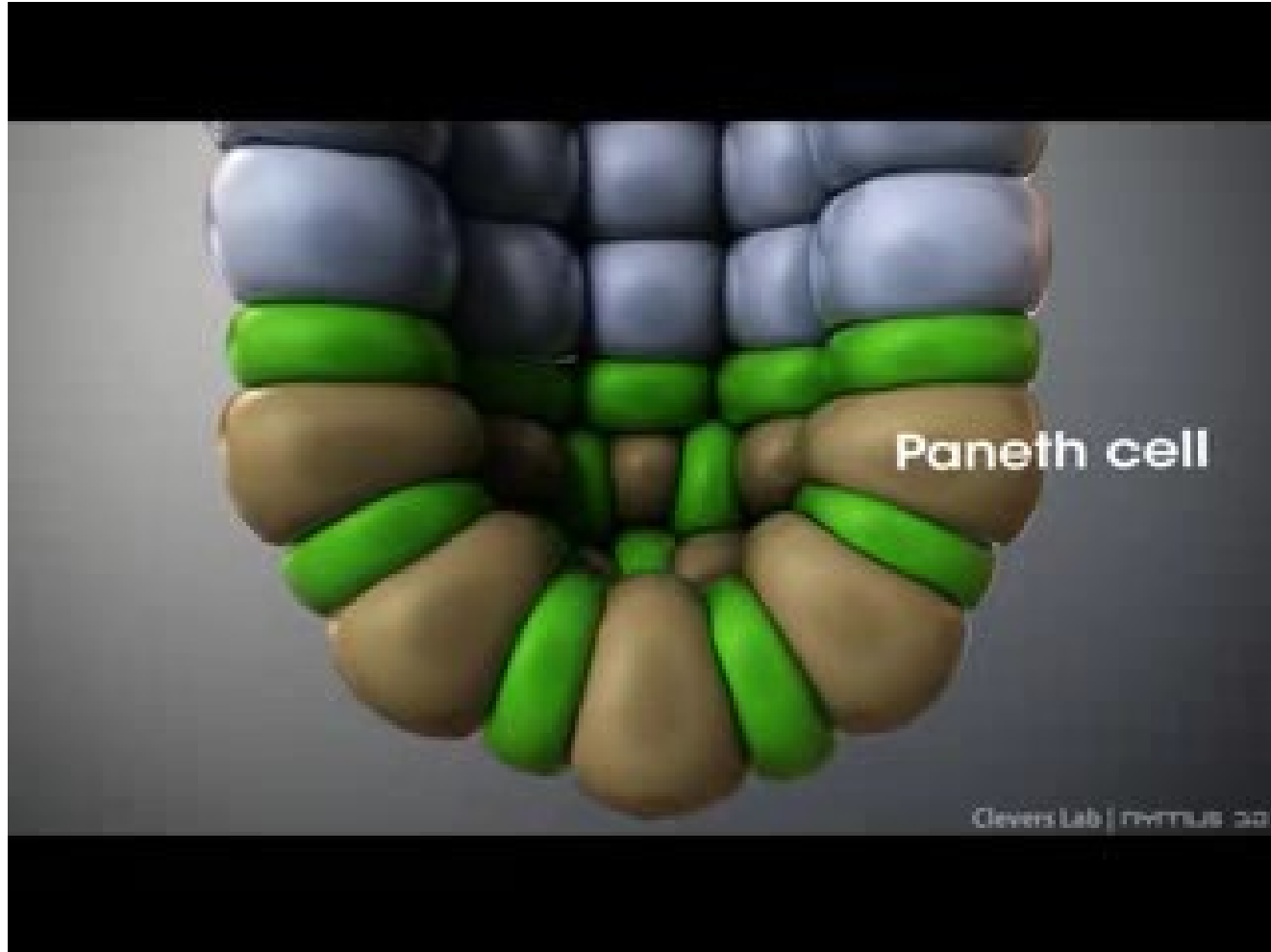
2006: kmenové buňky definovány jako „label-retaining cells“

- tj. jako buňky, které se nedělí

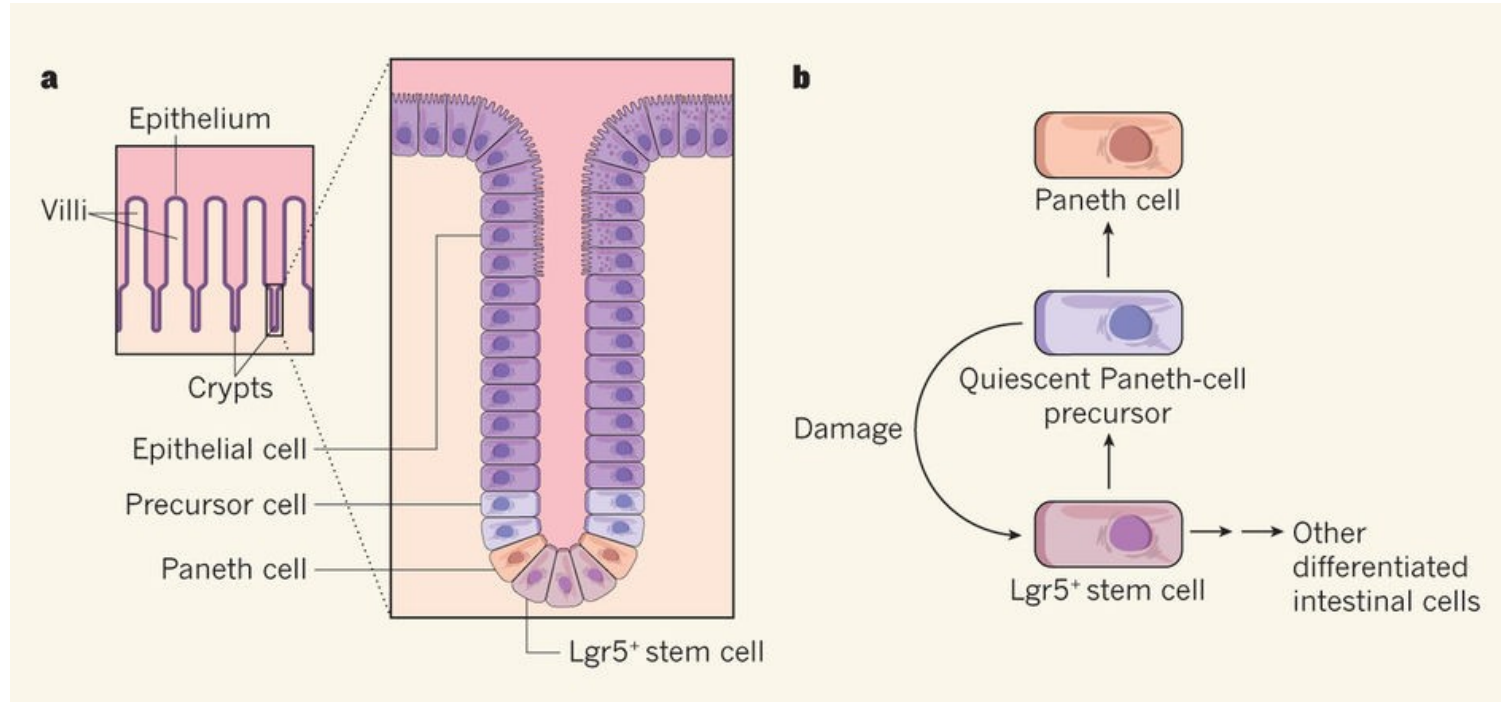
Co tedy jsou „label-retaining cells“?



Nedělicí se zásobárna buněk (DII1+) pro případ poškození a regenerace:



Nedělicí se zásobárna buněk pro případ poškození a regenerace:



a, The intestinal epithelium follows the distinct contours of villus–crypt units in the intestine. **b**, Normally, *Lgr5*-expressing stem cells (*Lgr5*⁺) lead to the production of precursor cells that further differentiate into the various types of crypt epithelial cell. Buczacki *et al.*¹ report that precursors of one type of differentiated intestinal cell, Paneth cells, can persist for several weeks in a quiescent state before maturing into Paneth cells. Intriguingly, these quiescent precursors can revert back into *Lgr5*⁺ stem cells following crypt damage.

Role kmenových buněk v rozvoji nádoru

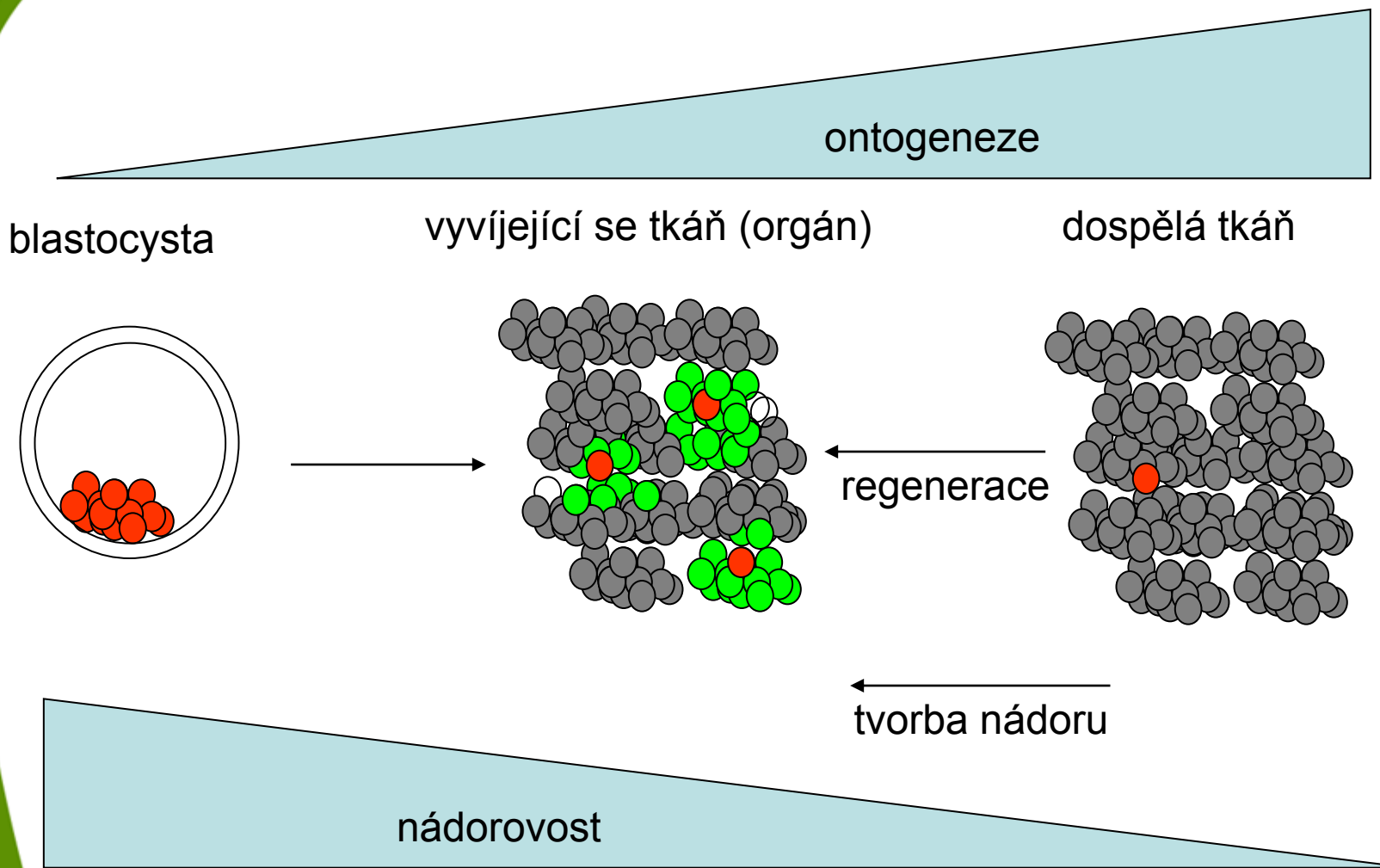
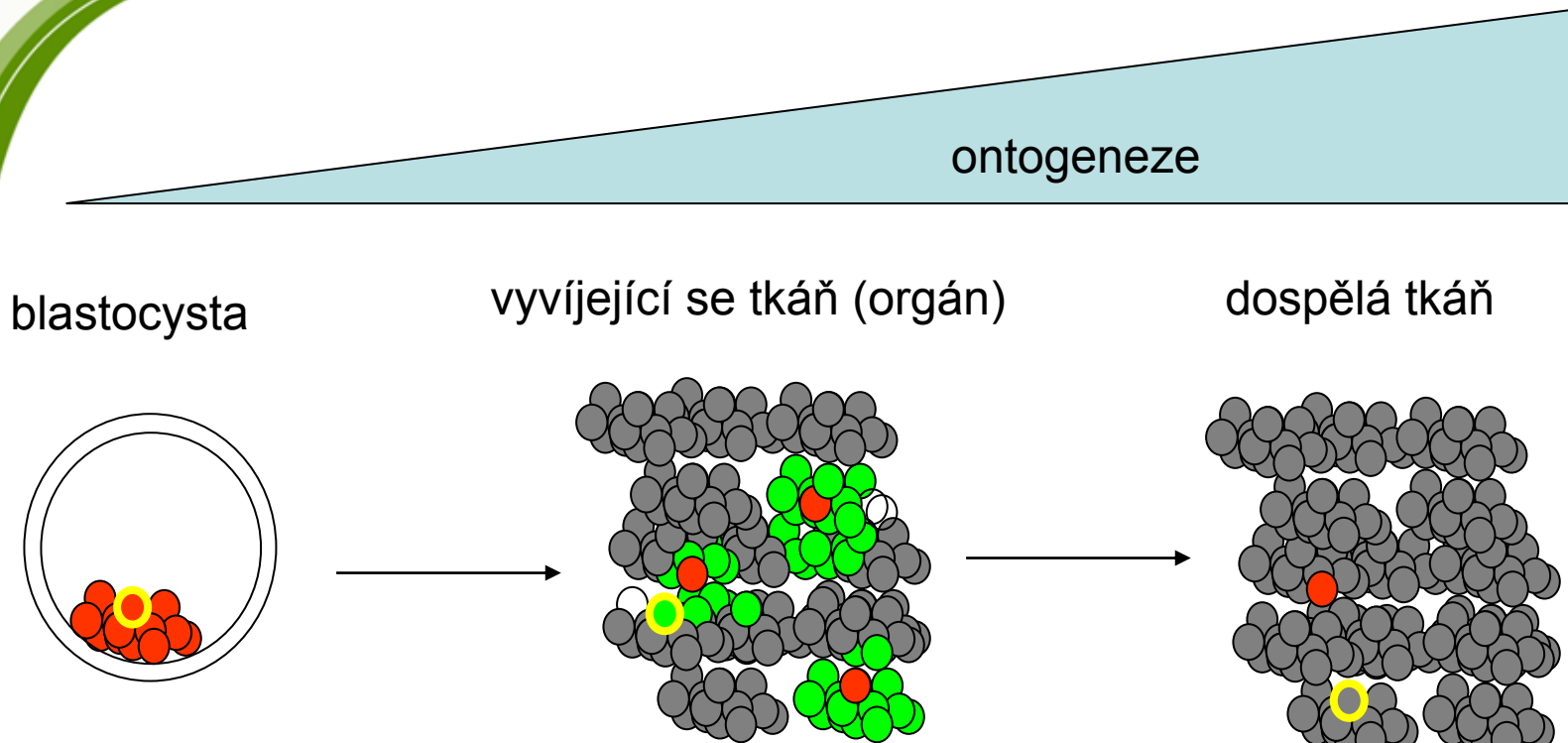


Table 2 Hh and Wnt pathways in cancer

Tissue	Tumour	Evidence of pathway involvement	References
Hh pathway			
Brain	Medulloblastoma	Tumorigenesis by inactivation of <i>PTCH</i> ; allograft and cell-line growth inhibition by cyclopamine; inhibition of autochthonous tumour growth by synthetic small molecule antagonist	37, 81; reviewed in 6
		Tumorigenesis by inactivation of <i>Su(fu)</i>	86
	Glioma	<i>Gli</i> amplification; growth inhibition of some cell lines by cyclopamine	87, 88
Skin	Basal cell carcinoma	Tumorigenesis by inactivation of <i>PTCH</i> ; <i>in vivo</i> tumorigenesis by expression of activating form of <i>SMO</i> or by <i>Shh</i> overexpression and <i>in vitro</i> growth inhibition by synthetic Hh pathway antagonist; inhibition of human tumour growth topical cyclopamine	82, 83; reviewed in 6
Muscle	Rhabdomyosarcoma	Tumorigenesis by inactivation of <i>PTCH</i>	reviewed in 6
Oesophagus	Adenocarcinoma	Cell-line growth inhibition by cyclopamine, Hh blocking antibody	42
Stomach	Adenocarcinoma	Cell-line growth inhibition by cyclopamine, Hh blocking antibody	42
Pancreas	Adenocarcinoma	Xenograft and cell-line growth inhibition by cyclopamine, Hh blocking antibody; tumour initiation (in mouse) by <i>Shh</i> overexpression	42, 43
Biliary tract	Adenocarcinoma	Xenograft and cell-line growth inhibition by cyclopamine, Hh blocking antibody	42
Lung	Small-cell lung cancer	Xenograft and cell-line growth inhibition by cyclopamine, Hh blocking antibody	41
Prostate	Adenocarcinoma	Xenograft and cell-line growth inhibition and suppression of metastasis by cyclopamine; increased xenograft growth by <i>Shh</i> and <i>Gli</i> overexpression	29, 89, 90
Bladder	Urothelial carcinoma	Increased tumour induction (in mouse) by alkylating agent in <i>Ptch</i> heterozygote	91
Oral cavity	Squamous cell cancer	Growth inhibition of cell lines by cyclopamine;	92
Wnt pathway			
Colon	Adenocarcinoma	Tumorigenesis by inactivation of APC, Axin; tumorigenesis by stabilization of β -catenin; epigenetic inactivation of SFRPs	47; reviewed in 45
Liver	Hepatoblastoma	Tumorigenesis (in mouse) by inactivation of APC and by stabilization of β -catenin	reviewed in 45
Blood	Multiple myeloma	Cell-growth inhibition by dominant negative TCF4; growth stimulation by Wnt ligand	93
Hair follicle	Pilomatricoma	Tumorigenesis (in mouse) by overexpression of β -catenin	reviewed in 45
Bone	Osteosarcoma	<i>Dkk3</i> and <i>LRP5</i> expression inhibits tumour cell growth <i>in vitro</i>	94, 95
Lung	Non-small-cell carcinoma	Apoptosis and cell-growth inhibition by short interfering RNA and a blocking antibody against Wnt2	96
Pleura	Mesothelioma	Apoptosis and cell-growth inhibition by transfection of SFRP	97

Emphasis is placed on functional data showing a requirement for pathway activation in tumour formation and/or tumour cell growth. (See Fig. 1 and text for gene abbreviations.)

Klasické morfogenetické dráhy (Wnt, Hh, Notch a další) regulují regeneraci, tkáňové specifické kmenové buňky i nádory



Počet mutací nutných pro vznik nádoru: 0

nádorovost

Teratomy

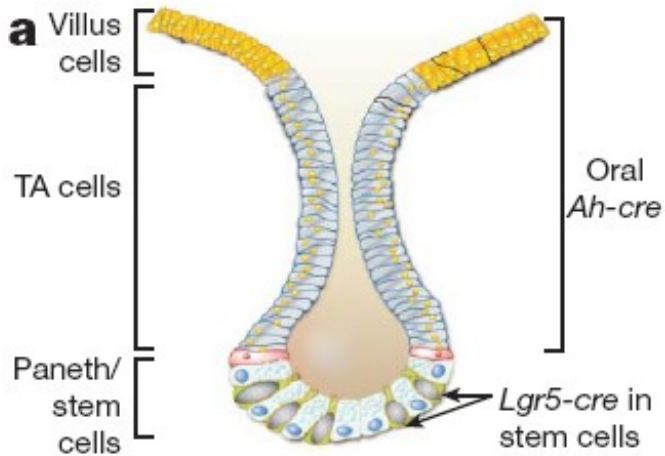


Klasické morfogenetické dráhy (Wnt, Hh, Notch a další) regulují regeneraci, tkáňové specifické kmenové buňky i nádory

Je to pravda?

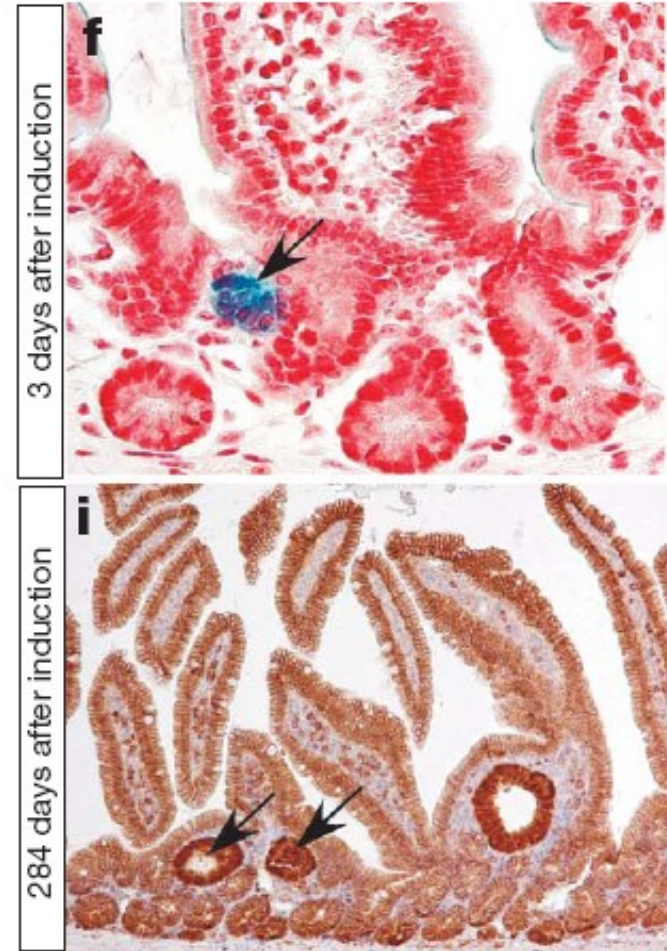
Experimentální důkaz:

Tkáňově specifický knockout nádorového supresoru APC

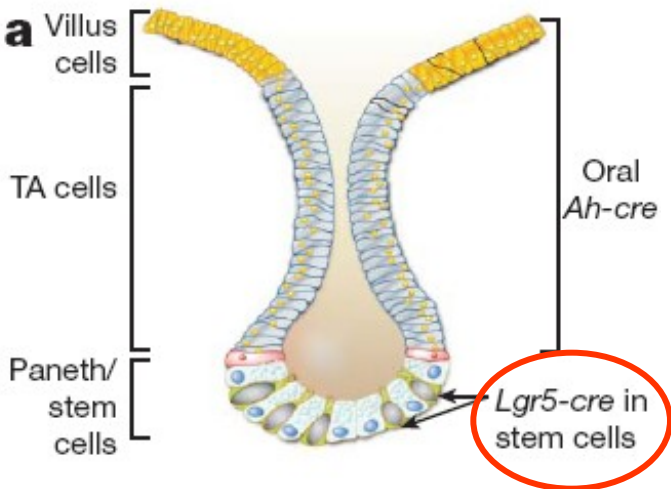


Zkřížení s APC flox/flox myšima + tamoxifen

Vznik malých adenomů, které neprogradují



Nekontrolovaná aktivace kmenových buněk má fatální následky



Zkřížení s APC flox/flox myšima + tamoxifen

Rychlý vznik adenomů a nádorů

NATURE | Vol 457 | 29 January 2009

